NASA TECHNICAL MEMORANDUM

NASA TM X-3549

PRELIMINARY FLIGHT MEASUREMENTS OF THE BUFFET CHARACTERISTICS OF PROTOTYPE LIGHTWEIGHT FIGHTER AIRCRAFT
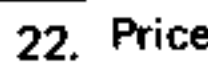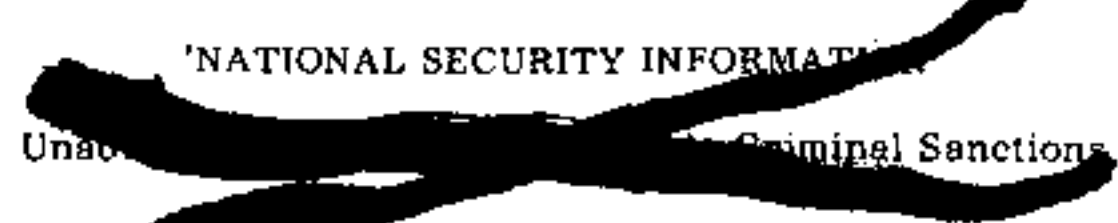
Edward L. Friend and Neil W. Matheny

Dryden Flight Research Center
Edwards, Calif. 93523

NATIONAL AERONAUTICS AND SPACE ADMINISTRATION · WASHINGTON, D. C. · MAY 1977

1. Report No. NASA TM X-3549	2. Government Accession No.	3. Recipient's Catalog No.
4. Title and Subtitle PRELIMINARY FLIGHT MEASUREMENTS OF THE BUFFET CHARACTERISTICS OF PROTOTYPE LIGHTWEIGHT FIGHTER AIRCRAFT		5. Report Date May 1977
		6. Performing Organization Code
7. Author(s) Edward L. Friend and Neil W. Matheny		8. Performing Organization Report No. H-924
		10. Work Unit No. 505-11-27
9. Performing Organization Name and Address NASA Dryden Flight Research Center P. O. Box 273 Edwards, California 93523		11. Contract or Grant No.
		13. Type of Report and Period Covered Technical Memorandum
12. Sponsoring Agency Name and Address National Aeronautics and Space Administration Washington, D. C. 20546		14. Sponsoring Agency Code

15. Supplementary Notes

16. Abstract

Selected maneuvers during the initial flight tests of prototype YF-16 and YF-17 lightweight fighter aircraft were analyzed to investigate their buffet and wing rock characteristics. Test Mach numbers ranged from approximately 0.62 to 0.96, with altitudes varying from 9144 meters (30,000 feet) to 12,192 meters (40,000 feet). Buffet intensity characteristics for both automatically scheduled and manually positioned fixed flap configurations, buffet frequency content, and aircraft wing rock characteristics are discussed, and pilot comments related to airplane response and handling are presented. To assist in quantifying the evaluation, comparisons are made with a current aircraft of similar configuration.

17. Key Words (Suggested by Author(s)) Lightweight fighters Buffet Wing flow separation Strakes Maneuver flaps Wing rock Vortex systems (forebody strakes)	18. Distribution Statement U. S. Government and Contractors only Category: 08

19. Security Classif. (of this report) (redacted)	20. Security Classif. (of this page) Unclassified	21. No. of Pages 49	22. Price

PRELIMINARY FLIGHT MEASUREMENTS OF THE BUFFET CHARACTERISTICS

OF PROTOTYPE LIGHTWEIGHT FIGHTER AIRCRAFT

Edward L. Friend and Neil W. Matheny
Dryden Flight Research Center

SUMMARY

The first flight evaluation of the YF-16 and YF-17 aircraft included an evaluation of the buffet and wing rock characteristics of these aircraft. Test Mach numbers ranged from approximately 0.62 to 0.96. Data were taken from windup-turn maneuvers at altitudes from approximately 9144 meters (30,000 feet) to 12,192 meters (40,000 feet). The aircraft underwent such modifications as changes in flap scheduling and augmentation gains during the test period; therefore, the data presented do not necessarily represent the optimum configuration.

At subsonic speeds, the buffet intensity rise boundaries were higher than those of other current aircraft. At transonic speeds, the boundaries were comparable to or higher than those of a similar low aspect ratio thin-winged aircraft. Significantly higher normal-force coefficients were obtainable in maneuvering flight than with most current aircraft. The scheduled flap deflections and forebody strakes on both aircraft were effective in reducing buffet intensities at high angles of attack. A mild-to-moderate wing rock condition existed for both aircraft over the Mach number range tested. The fixed flap deflection data revealed that additional refinements in flap scheduling would further improve the aircrafts' buffet characteristics. The data also showed that the wing rock boundary for the YF-17 aircraft could be raised with improved flap deflection scheduling; comparable data were not available for the YF-16 airplane.

INTRODUCTION

The maneuverability of high performance fighter aircraft in the transonic speed regime is being critically examined, since flight at the high load factors necessary for combat at these conditions necessitates the use of high angles of attack and lift coefficients. Thus, the associated buffet characteristics are also of vital concern in the development of modern fighter technology.

The maneuverability and performance of fighter aircraft at transonic speeds (Mach 0.85 to 1.00) are limited by unsteady flow separation phenomena, which are triggered by shock and boundary-layer interactions. Many flight test and wind tunnel studies have been conducted to determine the buffet characteristics and resulting handling qualities deficiencies of current aircraft. These studies are documented in references 1 to 7.

Various methods have been used to minimize shock-induced boundary-layer separation. One method is to incorporate supercritical airfoils. The capability of supercritical airfoils to delay shock-induced separation for wing thickness ratios from 9 percent to 17 percent has been well established from wind tunnel and flight experiments (ref. 8). Another approach is to use thin wings incorporating flaps (ref. 9).

Recent flight studies have established the buffet characteristics of several wing geometries that incorporate leading- and trailing-edge flaps as maneuvering devices. The use of flaps to vary wing camber has been effective in delaying flow separation to higher lift coefficients and in reducing such handling qualities deficiencies as wing rock (refs. 1, 2, 4, and 5).

The design approach used for the YF-16 and YF-17 lightweight fighters was to incorporate forebody strakes (leading-edge extensions) in thin cambered wings of moderate aspect ratio and sweep and to provide an automatic flap deflection schedule. The separation-induced vortex flows generated by strakes have successfully been used to provide aerodynamic advantages at high angles of attack, a subject that warrants extensive study. For example, wind tunnel studies have indicated that tailored strakes result in gains in incremental lift and reductions in buffet intensity (ref. 6).

The prototype lightweight fighter flight test program provided an opportunity to perform a preliminary evaluation of two recently designed aircraft which incorporated new design features to improve performance at high lift coefficients. A quantitative buffet analysis of both aircraft was performed during the first flights in the evaluation program. The aircraft underwent control system and flap deflection schedule modifications during the program; therefore, the data presented do not necessarily represent the optimum configuration. The results are presented in terms of buffet intensity characteristics, frequency content, wing rock characteristics, and pilot comments concerning airplane response and handling. Data are presented for both scheduled and fixed flap deflections. Comparisons are made with a current operational aircraft of similar configuration to assist in quantifying the evaluation. Some wind tunnel results are presented to permit the comparison of the buffet and aerodynamic performance characteristics of the lightweight fighter configurations with and without forebody strakes.

SYMBOLS AND ABBREVIATIONS

Physical quantities in this report are given in the International System of Units (SI) and parenthetically in U.S. Customary Units. The measurements were taken and the calculations were made in U.S. Customary Units. Factors relating the two systems are presented in reference 10.

$a_{n_{cg}}$ normal acceleration at center of gravity, g

$a_{n_{cp}}$ normal acceleration at cockpit, g

$a_{n_{wt}}$ normal acceleration at wingtip, g

B_m bending moment at wing root, m-N (in-lb)

$b/2$ airplane semispan, m (ft)

C_{N_A} airplane normal-force coefficient, $\dfrac{a_{n_{cg}} W}{\bar{q}S}$

C_{W_B} model root mean square bending-moment coefficient, $\dfrac{2\sigma_{B_m}}{\bar{q}Sb/2}$

F_Y lateral stick force, N (lb)

M Mach number

PCM   pulse code modulation

p roll angular velocity, deg/sec

$\bar{q}$ dynamic pressure, N/m^2 (lb/ft^2)

$\bar{q}_{ref}$ reference dynamic pressure, used for normalizing unsteady acceleration and bending-moment data, N/m^2 (lb/ft^2)

r yaw angular velocity, deg/sec

rms   root mean square

S wing area, m^2 (ft^2)

t time, sec

W airplane weight, N (lb)

α indicated angle of attack, deg

β indicated angle of sideslip, deg

δ control surface deflection, deg

σ root mean square value of buffet component of associated quantity

$\bar{\sigma}$ normalized value of buffet component, $\dfrac{\sigma}{\overline{q/\bar{q}}_{ref}}$

Φ power spectral density of buffet component of associated quantity

Subscripts:

a aileron

a_h differential horizontal tail

bir buffet intensity rise

le leading edge

max maximum

r rudder

te trailing edge

wro wing rock onset

AIRPLANE DESCRIPTION

The YF-16 and YF-17 lightweight fighter prototypes are single-place midwing aircraft that carry two AIM-9E missiles on the wingtips in the basic configuration (fig. 1).

The YF-16 airplane has a single F100-PW-100(2) turbofan engine with afterburner in conjunction with a normal shock inlet located under the forward fuselage. The airplane incorporates a forward fuselage strake, an all-movable horizontal stabilizer, programed leading-edge flaps (which are used as maneuvering surfaces), trailing-edge flaperons, a single vertical stabilizer, and a blended wing-fuselage. The trailing-edge flaperons are not used as maneuvering surfaces. The aircraft's combat gross weight is approximately 80.1 kilonewtons (18,000 pounds).

The YF-17 airplane has two YJ101-GE-100 low bypass ratio turbojet engines with afterburner. One air inlet is located under each wing next to the fuselage. The airplane incorporates forward fuselage strakes with boundary-layer bleed slots, an all-movable horizontal stabilizer, programed leading- and trailing-edge flaps (both of which are used as maneuvering surfaces), conventional ailerons, and twin canted vertical stabilizers. The aircraft's combat gross weight is 97.9 kilonewtons (22,000 pounds).

Wing Planforms

The wing geometries of the lightweight fighters and a similar currently operational aircraft, the F-5A airplane, are shown in figure 2. Table 1 contains details of the wing geometries and shows that the lightweight fighters are similar to the F-5A airplane in leading-edge sweep, aspect ratio, and thickness-to-chord ratio. The most obvious difference between the configurations is that the lightweight fighters have much larger forebody strakes. The forebody strakes of the YF-16 and YF-17 aircraft are similar in size, but there are some differences in planform and camber; the cross-sectional camber is significantly greater for the YF-17 airplane. The YF-17 strake also has forward fuselage boundary-layer bleed slots (fig. 2).

The leading-edge flaps are essentially full span on all three configurations. The YF-16 airplane has a 60-percent semispan flaperon, and the YF-17 airplane has a more conventional trailing-edge flap and aileron configuration.

Control Systems

The YF-16 control system is a pure analog fly-by-wire system that incorporates a limited-displacement force-sensing sidestick controller. The longitudinal control augmentation system is a command system that incorporates angle of attack and normal load factor limiting circuits. The lateral control augmentation system, which is also a command system, activates both the differential tail and the flaperons and has an aileron-to-rudder interconnect.

The YF-17 airplane has a mixed mechanical and fly-by-wire control system with a conventional center-stick controller. The elevons, rudders, and flaps are mechanically controlled, but the ailerons are controlled fly by wire. The longitudinal and lateral control augmentation systems are both command systems. The lateral control augmentation system operates only through the ailerons. It has separate aileron-to-rudder and differential-tail-to-rudder interconnects.

The maneuver flaps of both aircraft are automatically scheduled as functions of Mach number and angle of attack. The flap deflection schedules are shown in figures 3(a) and 3(b) for the YF-16 and YF-17 airplanes, respectively. The deflections of the leading- and trailing-edge flaps are scheduled with angle of attack and Mach number for the YF-17 airplane, and the deflection of the leading-edge flap for the YF-16 airplane is scheduled similarly. The flap deflections measured for both aircraft in flight are shown in figure 4. These data were obtained during typical windup-turn maneuvers. Some differences between the actual and programed flap deflections appear. Some of the differences were attributed to changes in Mach number during the runs and some were due to structural deformations that caused the actual flap deflections to be less than scheduled. For this reason, a second flap deflection schedule was mechanized for the YF-17 airplane to deflect the flaps at a lower angle of attack for each Mach number. Most of the data presented are for the original schedule.

INSTRUMENTATION AND DATA ACQUISITION SYSTEMS

The instrumentation and data acquisition systems for both airplanes were installed and maintained by the aircraft manufacturers and included standard air data, airplane response, and control position transducers. The transducers used for the buffet evaluation of the YF-16 airplane consisted of bending, shear, and torsion strain gage bridges at the wing root and a normal-force accelerometer at the cockpit. The buffet instrumentation on the YF-17 airplane consisted of five normal-force accelerometers, two on each wingtip and one at the cockpit.

The data acquisition systems for both aircraft were of the pulse code modulation (PCM) type. The sample rates were approximately 39 samples per second for the YF-16 airplane and 139 samples per second for the YF-17 airplane. The YF-16 data acquisition system included an FM recording capability in addition to the PCM system. The flight tapes were calibrated and instrumentation corrections were applied by the Air Force Flight Test Center at Edwards Air Force Base to produce a tape in engineering units. The engineering units tape was then converted to a format compatible with the NASA Dryden computer, and the data were processed using NASA Dryden programs.

FLIGHT TEST CONDITIONS

Windup-turn maneuvers were performed over the subsonic and transonic Mach number region at altitudes from 9144 meters (30,000 feet) to 12,192 meters (40,000 feet). Many of the maneuvers were performed for other reasons (such as systems and performance evaluation), and some were considered to be marginal for buffet analysis because of the rapidity with which the maneuvers were performed. Large changes in Mach number occurred during many of the windup-turn maneuvers, preventing the evaluation of some Mach number trends. A matrix of flap deflections was flown late in the program for wing rock and buffet evaluations; the Mach numbers and accompanying flap deflections are shown in table 2.

DATA INTERPRETATION AND ANALYSIS

Typical analog time histories of windup turns used in the buffet analysis, including root mean square (rms) values of buffet loads, are shown in figures 5 and 6. Figure 5 shows two maneuvers for the YF-16 aircraft—the first with the scheduled leading-edge flap deflections and the second with a zero flap deflection (the clean configuration). The first significant event that occurs with increasing angle of attack is buffet intensity rise. The actual determination of buffet intensity rise is discussed later in this section. The buffet intensity rise point is not obvious in all of these time histories because the increase in angle of attack is irregular.

The second event is wing rock onset, which is the point where a distinct and uncommanded roll rate begins. The scheduled leading-edge flap maneuver for the YF-16 airplane (fig. 5(a)) shows few lateral control inputs. However, the clean

configuration maneuver (fig. 5(b)) is accompanied by increased lateral control activity after wing rock onset because the pilot is attempting to control the wing rock. The increased rudder activity at a time of 9 seconds in figure 5(a) and a time of 10 seconds in figure 5(b) is attributed to the aileron-to-rudder interconnect.

Wing rock onset, like buffet intensity rise, is a phenomenon of flow separation. High roll rates usually produce yaw excursions through aerodynamic lateral-directional coupling, and the resulting sideslip excursions cause large miss distances (radial mil tracking errors) during aircraft tracking evaluations (refs. 5 and 7). However, for the YF-16 aircraft there is little sideslip after wing rock onset.

Figure 6 shows a similar set of windup-turn maneuvers for the YF-17 aircraft. The magnitudes of the roll rates and sideslip after wing rock onset are slightly higher than for the YF-16 airplane. However, the lateral stick inputs indicate that the pilot is partly responsible for driving the wing rock (that is, amplifying the roll rate).

An explanation of the method used to calculate the rms values of the buffet loads is necessary for a full understanding of the method used to determine the response of the wing structure to separated flow. The normal acceleration and load traces show two kinds of variation during buffeting. One is slow and steady and represents maneuvering. Superimposed on this variation is a rapidly fluctuating load variation which represents buffet. The fluctuating loads were analyzed for continuous 1-second time segments during periods of increasing angle of attack. Computer programs were used to analyze the digital data from the periods chosen for analysis. First, the oscillating loads were separated from the maneuver loads, using a third-order Butterworth high-pass filter with a 3-hertz corner frequency (refs. 11 and 12). Then the rms values of the oscillating loads for each period were found, and those values were defined as buffet loads.

Power spectral density techniques were used to indicate the power and the frequency distribution of the buffet parameters. Periods of approximately 3 consecutive seconds were analyzed at times of high buffet intensity and approximately constant angle of attack. Periods of this type were chosen in order to confine the analysis to intervals of high buffet sensor output and fairly constant sensor response.

Figure 7 shows typical normal-force and buffet intensity characteristics. Buffet intensity rise was defined as the point at which $\bar{\sigma}_{a_{n_{wt}}}$ increased rapidly. Some flight reports (ref. 3, for example) refer to buffet onset. In those reports, buffet onset was interpreted as being indicated by the first rapid fluctuation in the normal acceleration or wing bending-moment trace. However, in some cases a low degree of wing separation (that is, buffet onset) occurs at a low angle of attack without a significant increase in separation until a higher angle of attack is reached (ref. 5). The buffet intensity rise technique is apparently more consistent in determining the beginning of significant separation, and for that reason the buffet intensity rise technique was used in this study. In general, only fairings are shown for the balance of the report to facilitate the data presentation.

RESULTS AND DISCUSSION

The buffet intensity and wing rock characteristics of both lightweight fighters were determined with the flaps in the scheduled mode. In addition, the effects of fixing the flaps at off-schedule deflections, separate from and in combination with flaps in the scheduled mode, were investigated to permit the refinement of the flap deflection scheduling. However, the scarcity of data allowed only trends to be determined. Since the flight programs for the lightweight fighters were conducted separately and with some differences in objective, the data for each aircraft are presented separately and segregated according to flap mode. In some cases, trends with Mach number are not discussed because of the large changes in Mach number during the maneuvers.

Comparisons are made with data for an F-5A airplane. A description of the F-5A flight program and some of the data from it are published in reference 5. Some of the F-5A data presented herein were obtained during that program but have not been published previously.

Buffet Intensity Rise Boundaries

Scheduled flaps.—The variations in the boundary for buffet intensity rise are shown in figures 8(a) and 8(b) for the flap schedules used on the YF-16 and YF-17 aircraft, respectively. The boundaries are shown in terms of airplane normal-force coefficient and airplane angle of attack as a function of Mach number. For both aircraft, the normal-force coefficient for buffet intensity rise tends to decrease as speed increases from subsonic to transonic. At high transonic speeds, the boundary rises rapidly as supersonic flow is approached. The flap deflections at buffet intensity rise in the Mach number range from 0.85 to 0.93 are essentially zero, and the resulting boundary is similar to that of nonflapped supersonic aircraft (ref. 2). At Mach numbers below 0.85, the effective camber increases resulting from the large flap deflections on the lightweight fighters increase the buffet intensity rise boundary to a significantly higher normal-force coefficient.

It has long been recognized that increased camber and thickness-to-chord ratio have favorable effects on aircraft buffet characteristics at subsonic Mach numbers, where leading-edge flow separation occurs as stall is approached (ref. 6). Recent flight programs (refs. 1, 2, 4, and 5) have shown that moderate flap deflections have similar beneficial effects at transonic speeds, where shock-induced flow separation occurs. A few maneuvers were performed on the YF-17 airplane with a modified flap deflection schedule (flaps deflected at a lower angle of attack). The effects on the buffet intensity rise boundary are shown in figure 8(b). These data show that a small deflection of the trailing-edge flap has small effect on α_{bir} but increases $C_{N_{A_{bir}}}$ by approximately 0.1. Physically, deflecting the trailing-edge flap loads the inboard portion of the wing, permitting a higher lift coefficient to be reached before the angle of attack for shock-induced flow separation occurs. The trailing-edge flap is approximately 46 percent of the wing semispan (table 1).

The maximum depth of buffet penetration for these maneuvers is shown in relation to the normal-force coefficient and angle of attack boundaries for buffet intensity rise. The depths of buffet penetration of the aircraft discussed in references 1 to 5 in terms of C_{N_A} and α are summarized and shown as bandwidths.

The lightweight fighter and the aircraft boundaries from references 1 to 5 do not necessarily represent the operational limits of the aircraft; however, the boundaries for the lightweight fighters are at considerably higher normal-force coefficients.

Fixed flaps.—A few windup-turn maneuvers were performed with fixed flap deflections with both the YF-16 and YF-17 aircraft to determine whether the aircrafts' buffet characteristics could be improved with different flap scheduling. The effects of separate and combined deflections of the leading- and trailing-edge flaps on the normal-force coefficient for buffet intensity rise are shown in figures 9 and 10.

The buffet intensity rise boundary for fixed deflections of the leading-edge flap with a zero trailing-edge flap deflection is shown in figure 9(a) for approximate Mach numbers of 0.80, 0.85, and 0.95 for the YF-16 aircraft. The results indicate that moderate deflections of the leading-edge flap produce significant increases in the normal-force coefficient for buffet intensity rise. The somewhat meager data are augmented by the scheduled flap data from figure 8(a) to assist in the formation of a fairing. At Mach 0.80, the scheduled flap deflection results in the highest $C_{N_{A_{bir}}}$.

For Mach 0.85, a fixed leading-edge flap deflection of 5° results in a slightly higher $C_{N_{A_{bir}}}$ than the scheduled flap deflection. However, there are insufficent data to determine the optimum flap deflection. The fixed flap data at Mach 0.95 are also considerably higher than the scheduled flap data point. Large deflections of the leading-edge flap affect the boundary detrimentally for all Mach numbers for which there are data, suggesting that these flap deflections cause flow separation on the upper and possibly also the lower surface of the wing.

The advantage of deflecting the trailing-edge flap on the YF-16 airplane (although trailing-edge flap deflection is not one of the aircraft's operational features) is shown in figure 9(b). Only a few data points were obtained during these tests, for which the leading-edge flap was in the scheduled mode. For comparison purposes, the fairings for Mach 0.80 and Mach 0.85 from figure 9(a), which are for deflected leading-edge flaps only, are also shown. The combination of leading- and trailing-edge flap deflections resulted in some gains compared with the results of deflecting the leading-edge flaps only. Because of the lack of data and the sensitivity of the flow to airfoil geometry, optimum settings cannot be determined from this set of data.

The effects of separate and combined flap deflections on the normal-force coefficient for buffet intensity rise are shown in figure 10 for the YF-17 aircraft at Mach numbers of approximately 0.80 and 0.90. The data for Mach 0.90 (fig. 10(a)) indicate that, as would be expected, trailing-edge flap deflection is significantly more effective than leading-edge flap deflection in delaying buffet intensity rise.

Very few data points were available for Mach 0.80 (fig. 10(b)); however, trends similar to those for the Mach 0.90 data are apparent for moderate flap settings.

The results shown in figure 10 indicate that the buffet intensity rise boundary in figure 8(b) can be improved with a revised flap schedule.

Normal-Force and Buffet Intensity Characteristics

Scheduled flaps.—The normal-force and buffet intensity characteristics of both test aircraft are shown in figure 11 for the scheduled flap deflections. The normal-force curves for the YF-17 airplane (fig. 11(a)) show a slope change at approximately the same normal-force coefficient as for buffet intensity rise. The slope remains reduced through the higher angle of attack range, which is primarily the result of flow separation, large reductions in Mach number, and reductions in trailing-edge flap deflection. The offset and nonlinearity of the normal-force curves at low and moderate angles of attack are due primarily to the trailing-edge flap deflection schedule (fig. 3(b)). Because of large reductions in Mach number with increasing angle of attack for each windup-turn maneuver, the effects of Mach number cannot be evaluated.

The normal-force data for the YF-16 airplane (fig. 11(b)) are more linear than for the YF-17 airplane. The changes in slope and the offsets for this airplane are small and are due primarily to flow separation and Mach number variations. Both aircraft achieve higher normal-force coefficients than most current aircraft for similar flight conditions (fig. 8). The higher normal-force coefficients achieved by the YF-16 and YF-17 aircraft are thought to be due to the increased camber due to flap deflection and to favorable interactions between the strake-induced vortex flow and the wing flow. Reference 6 discusses wind tunnel studies which also showed that lift was increased by using strakes and flap deflection.

Buffet intensity for the YF-17 airplane is expressed in figure 11 as the rms value of wingtip normal acceleration. For the YF-16 airplane, it is expressed as the rms value of the wing root bending moment. The rms values of the YF-16 bending moment are divided by the maximum bending moment for each run, and thus may be interpreted as the percentage of the maximum load produced. The YF-16 buffet load does not exceed 3 percent of the maximum load. The results for both aircraft indicate a rather rapid buffet intensity rise at lower normal-force coefficients and a tendency to level off at higher values of C_{N_A}. This leveling off, which is discussed in more detail in a later section, may be attributed to the strakes. The effects of Mach number on the aircraft's buffet intensity characteristics cannot be determined because of the large changes in Mach number during the runs. Most current aircraft exhibit both higher rates of buffet intensity rise and higher absolute magnitudes of buffet loads than the lightweight fighter prototypes with increasing C_{N_A} (ref. 4). Thus, the favorable effects of the lightweight fighters' strakes and flap deflections are evident in their buffet as well as in their normal-force characteristics.

Fixed flaps.—Fixed flap studies were conducted by the manufacturers to investigate the effectiveness of using flap deflections in combination with forebody strakes for maneuver performance and to optimize the flap deflection schedule. These studies offered an opportunity to determine whether the trends for the YF-16 and YF-17

aircraft were similar to those reported in previous references for aircraft that utilized fixed leading- and trailing-edge flaps for maneuver enhancement.

Figures 12 and 13 present the normal-force and buffet intensity characteristics for fixed leading- and trailing-edge flap deflections for the YF-16 and YF-17 aircraft, respectively. Figures 12(a) to 12(c) show the YF-16 aircraft with a trailing-edge flap deflection of zero and several leading-edge flap positions at three Mach numbers. The normal-force curves show that at Mach 0.80 and Mach 0.85 a leading-edge flap deflection reduces the normal-force coefficient at low and intermediate angles of attack but tends to increase it at the higher angles of attack. This improvement at high angles of attack is not apparent at Mach 0.95.

The buffet intensity data for Mach 0.80 and Mach 0.85 show that a low leading-edge flap deflection (4°) increases the normal-force coefficient for buffet intensity rise but that an intermediate leading-edge flap deflection (14°) reduces the normal-force coefficient for buffet intensity rise. At Mach 0.95 (fig. 12(c)), gains are again shown for low flap deflections and there is no tendency for the intermediate flap deflection to cause the normal-force coefficient for buffet intensity rise to decrease. With a high leading-edge flap deflection (24°), there are no buffet-free regions at any Mach number, probably because of separation on the lower wing surface at low normal-force coefficients and on both surfaces at intermediate normal-force coefficients. At high normal-force coefficients, this large leading-edge flap deflection reduces buffet intensity.

Several maneuvers were flown at Mach 0.85 with the trailing-edge flaps fixed at deflections other than zero and with the leading-edge flaps in the scheduled mode. The data from these maneuvers are shown in figure 12(d). The level of C_{N_A} for a given angle of attack is increased moderately by deflecting the trailing-edge flap. Some reduction in buffet intensity is evident for a trailing-edge flap deflection of 8° at low and moderate values of C_{N_A} when compared with data for the zero trailing-edge flap deflection. The data for a trailing-edge flap deflection of 16° show essentially no gain. References 2 and 4 show similar gains for angles of attack less than or equal to 16° through the use of trailing-edge flap deflections.

Figures 13(a) and 13(b) show the effects of combined leading- and trailing-edge flap deflections at a Mach number of 0.80 for the YF-17 airplane. The data from the scheduled flap maneuver are shown for comparison. The combined flap deflection data show an increase in C_{N_A} at a given angle of attack and a reduction in buffet intensity, indicating that increasing the deflections of both the leading- and trailing-edge flaps would improve the airplane's flow separation characteristics.

The data shown in figure 13(c) are for three leading-edge flap deflections at Mach 0.90 for a zero trailing-edge flap deflection. The effects of leading-edge flap deflections at low and high angles of attack are similar to those shown for the YF-16 airplane (figs. 12(a) and 12(b)). At intermediate angles of attack, however, where the clean wing flow separates, leading-edge flap deflection results in significant gains.

The data from several combinations of leading- and trailing-edge flap deflections are compared with the data from the flap schedule in figure 13(d) at Mach 0.90. The figure shows significant improvements in the normal-force coefficient for buffet intensity rise and buffet intensity levels with combined flap deflections.

Comparison with current aircraft.—In assessing the buffet characteristics of a new aircraft, a comparison with the characteristics of an existing aircraft of similar configuration is useful in that it serves to quantify the evaluation. Figure 2 shows the similarity of the YF-16, YF-17, and F-5A wing geometries; the only significant difference is the small size of the F-5A strake. Various combinations of fixed leading- and trailing-edge flap deflections were tested in flight on the F-5A airplane (ref. 5). Deflecting the leading-edge flap 4° and the trailing-edge flap 12° was found to be optimum for transonic maneuverability for this configuration, and the data presented hereafter are for these flap deflections.

Figure 14 shows a comparison of the normal-force and buffet characteristics of the F-5A and lightweight fighter aircraft. The gains for the lightweight fighters are quite evident in comparison with the F-5A airplane. At Mach numbers below 0.86 (fig. 14(a)), the normal-force coefficients for buffet intensity rise for the lightweight fighters are higher than for the F-5A airplane. At the higher transonic speeds the buffet intensity rise boundaries are similar. The normal-force curves for the three aircraft at the initial Mach number of approximately 0.90 are similar at the low angles of attack (fig. 14(b)). At an angle of attack of approximately 12°, the slope of the F-5A normal-force curve changes greatly, suggesting extensive flow separation. The discussion in reference 5 implies that the F-5A airplane has a practical limit of $C_{N_A} = 1.00$ for maneuvering. The slope reductions in the normal-force curves for the lightweight fighters are definitely less than those shown for the F-5A airplane at the higher angles of attack.

A buffet intensity comparison reveals that buffet intensity rise for the lightweight fighters occurs at a higher normal-force coefficient than for the F-5A airplane and that buffet intensities for the lightweight fighters do not increase appreciably with further increases in C_{N_A}. The buffet intensities for the F-5A airplane show no signs of leveling off, however, and this is typical of most current aircraft (refs. 1 to 5). The improvements shown for the lightweight fighters can be attributed primarily to flap deflections and the use of forebody strakes (ref. 6).

Wing Rock Characteristics

Wing rock may be defined as an irregular and uncommanded rolling-yawing motion that prevents precise control. Wing rock onset, like buffet intensity rise, is a phenomenon of flow separation. Reference 5 shows that flap deflections improve both the buffet intensity rise boundary and the wing rock boundary. These tests, although not complete in Mach number and flap deflection coverage, provided an opportunity to determine the influence of flap deflections on the wing rock characteristics of one of the lightweight fighters.

Scheduled flaps.—Figure 15 illustrates the variation of the wing rock onset boundary for the YF-17 airplane with scheduled flaps in terms of normal-force coefficient, angle of attack, and Mach number. As is typical, the boundaries are high at subsonic speeds and decline rapidly as transonic speeds are approached. At transonic Mach numbers greater than 0.92, the boundary would be expected to rise in the same manner as the boundary for buffet intensity (fig. 8).

Figures 16(a) and 16(b) show the differences in the wing rock phenomenon at subsonic and transonic Mach numbers. In these time histories wing rock onset was interpreted as being indicated by the first major oscillation in roll rate. The time history for Mach 0.60 shows a high angle of attack for wing rock onset and significant roll rate and sideslip excursions after wing rock onset. The high roll rates, through aerodynamic lateral-directional coupling, produce the large sideslip excursions, which in turn cause large miss distances during air-to-air tracking (ref. 7).

The time history for Mach 0.85 shows a moderate angle of attack for wing rock onset, with moderate oscillations in roll rate and low excursions in sideslip after wing rock onset.

The data available were too few to permit the documentation or analysis of the wing rock characteristics of the YF-16 airplane. However, the time histories discussed previously (for example, fig. 5) indicate mild wing rock with limited sideslip excursions.

Fixed flaps.—The effects of separate and combined deflections of the leading- and trailing-edge flaps on the normal-force coefficient for wing rock onset at a Mach number of approximately 0.80 are shown in figure 17 for the YF-17 airplane. The data indicate that the trailing-edge flap is more effective than the leading-edge flap in delaying wing rock onset at this flight condition. In addition, a comparison with figure 15 shows that wing rock onset occurs at a higher normal-force coefficient with the combined flap deflections than with the scheduled flaps.

Wing Structural Response Characteristics

There was some doubt about whether the PCM data acquisition system on the YF-16 airplane was adequate for a buffet evaluation because its sample rate was so low (39 samples per second). However, a power spectral density analysis using a Fourier analyzer indicated the same wing frequency distribution at excitation frequencies up to 32 hertz for data from both the YF-16 FM tape and the PCM system. This analysis substantiated the validity of the results obtained by using data from the PCM system.

Power spectral density distributions of the wing buffet intensities determined from the PCM systems of both aircraft are presented in figure 18 for a Mach number of approximately 0.85. The peaks in the data correlate well with the approximate values of the wing natural frequencies (shown as vertical lines) as determined by the manufacturer in ground vibration tests.

The wing structures of both aircraft respond in the first symmetric wing bending mode. However, the frequency distribution $\Phi_{a_{n_{wt}}}$ for the YF-17 airplane shows significant power between 24 hertz and 36 hertz, whereas the Φ_{B_m} data for the YF-16 airplane show essentially no power above 10 hertz. Although the limited sample rate provided by the PCM system for the YF-16 airplane would prevent analysis at the higher frequencies from becoming apparent in any case, the FM results mentioned previously also indicate the absence of power above 10 hertz. Other aircraft besides the YF-17 airplane that use wingtip accelerometers have also been observed to have significant power at the higher wing frequencies. Previously published data (ref. 4) have shown that although the frequencies registered by wingtip accelerometers and wing bending-moment sensors do not display similar frequency content, the resulting buffet intensity characteristics are similar. The light structure of the wingtip and the bracket that holds the accelerometer may have contributed to the YF-17 response.

Cockpit Environment

The military specification for the flying qualities of piloted airplanes (MIL-F-8785B(ASG)) states: "Within the boundaries of the Operational Flight Envelope, there shall be no objectionable buffet which might detract from the effectiveness of the airplane in executing its intended missions". Buffet, as the pilot feels it, may stem from sources ranging from flow separation on the wing to vibrations originating from such things as structural excitation, engine duct noise, and moving machinery. Since the pilot is physiologically sensitive to certain frequency ranges, a power spectral density analysis of the cockpit environment is necessary to determine its acceptability.

Buffet intensities and power spectral densities of accelerations measured in the YF-16 and YF-17 cockpits are presented in figure 19. The data were obtained during windup-turn maneuvers from a normal-force accelerometer mounted on the seat rail. Results for the YF-17 aircraft (fig. 19(a)) show increasing levels of buffet at high normal-force coefficients with no tendency to level off. Pilots perceive the onset of buffet at approximately $\bar{\sigma}_{a_{n_{cp}}} = 0.02$ and generally accept levels up to approximately 0.10, a level of buffet considered to be moderate (ref. 9). The plot of power spectral density indicates the frequency of most of the power to be above 16 hertz. Some recent studies (ref. 13) indicate that frequency content is as important as intensity level to pilot comfort, and that human beings are most susceptible to the frequencies from 4 hertz to 12 hertz. The higher frequencies exhibited by the YF-17 airplane may therefore be unobjectionable.

Cockpit buffet intensities and a power spectrum for the YF-16 aircraft are shown in figure 19(b). A frequency distribution determined from the FM data was compared with the PCM results. (The analysis was similar to the one discussed previously.) Some power observed at frequencies above 15 hertz in the FM data does not show up in the PCM results in figure 19(b). However, the trends in the buffet intensity data

from the PCM system, which are generally substantiated by pilot comments, are believed to be realistic. The results indicate generally low cockpit buffet intensities for the test conditions shown.

Pilot Comments

The pilots who flew the YF-16 aircraft experienced light to moderate buffet in the cockpit at most high angle of attack flight conditions. Mild wing rock was occasionally observed at transonic speeds, particularly during sustained maximum power turns at Mach 0.90 and an altitude of 30,000 feet. Although there were some exceptions, wing rock was felt to be sufficiently mild to have little effect on gunsight tracking error. The apparently highly effective lateral control augmentation generated through the flaperons is believed to be responsible for suppressing most of the wing rock (ref. 14). However, it was impossible to check this effect, since the augmentation could not be turned off.

The pilots who flew the YF-17 aircraft experienced what they described as moderate buffet in the cockpit. They believed that the wing rock experienced could cause some degradation in tracking precision; however, there are no quantitative data to evaluate this.

During the initial fly-off stages of the flight program, both aircraft underwent considerable control system changes. These changes and the fact that many pilots flew the aircraft contributed to there being a variety of pilot comments. However, grouping the maneuvers that were similar and the flights that were made at similar stages of aircraft development helped in evaluating the pilot comments concerning buffet and wing rock.

Wind Tunnel Studies

The flight results discussed in the previous sections showed that improvements in aerodynamic performance resulted from deflecting the flaps. The effects of the forebody strakes could not be evaluated in flight, since the aircraft were not tested without strakes. Therefore, data from wind tunnel studies which evaluated models with and without forebody strakes (and with and without flap deflections) are included in this paper.

Figures 20 and 21 present unpublished wind tunnel results for a rigid 1/15-scale model of the YF-16 airplane and a rigid 8-percent-scale model of the YF-17 airplane. The YF-17 model deviated from scale in that it incorporated a slightly oversized wing.

The YF-16 model was tested in the NASA Langley 8-Foot Transonic Pressure Tunnel at a Reynolds number of 10.4×10^6 per meter (3.2×10^6 per foot). The effects of forebody strakes at Mach 0.80 are shown in figure 20(a). The flaps were not deflected, and the missiles and launchers were not included in these tests. These figures show an improvement in normal-force coefficient with the strakes on that begins at an angle of attack of approximately 8° and reaches a level of approximately 0.10 at the higher angles of attack. The buffet intensity coefficient,

C_{W_B}, which is discussed in reference 15, is slightly lower at low normal-force coefficients with the strakes off. At higher normal-force coefficients there is a small gain with the strakes on.

Figure 20(b) presents data for the YF-16 model with strakes, missiles, and launchers on and the flaps deflected. In general, the model's buffet intensity characteristics improve with the flaps deflected.

Figure 21 presents the normal-force characteristics of the YF-17 airplane with and without forebody strakes and with zero flap deflection. The data are unpublished and from wind tunnel tests made in the Calspan 8-Foot Transonic Wind Tunnel at a Reynolds number of 11.5×10^6 per meter (3.5×10^6 per foot). The advantage of having the strake is significantly greater at subsonic Mach numbers than at the transonic Mach numbers of 0.80 and 0.90. The data for Mach 0.60 show gains at angles of attack above 12°, with the increase in C_{N_A} reaching approximately 0.2 at the higher angles of attack. Similar but smaller gains are shown for Mach 0.80, and no real gains are evident for Mach 0.90.

Figure 22 presents oil-flow photographs for the 1/15-scale YF-16 model for the clean wing at Mach 0.90 with the forebody strakes on. The strakes are not visible in the photographs because fluorescent oil was applied only to the wing surfaces; however, the interaction of the wing and the vortex flow field due to the strakes is obvious, especially in regions of shock-induced separation. Figure 22(a) shows the flow pattern for an angle of attack of 4.7° and reveals a tight, well-defined vortex core on the inboard portion of the wing. Also shown are a mild shock near the leading edge and a strong normal shock on the rear section of the wing parallel to the trailing edge. The photograph reveals that the vortex flow field and the shock waves have little influence on the direction of flow across the wing. There is no flow separation at this angle of attack.

Figure 22(b) shows the flow pattern for an angle of attack of 10.8°. The region of vortex flow is well defined, and shock-induced separation has begun to occur. The vortex pattern at this angle of attack has changed from a tight well-defined core to a larger, expanding, rotating field that generates extensive inward flow above the wing surface. The inward flow, in turn, apparently inhibits flow separation on the outboard wing panel. Shock-induced flow separation exists at the leading and trailing edges of the wing and at the wingtip. The region of separated flow on the rear section of the wing appears to have been limited and prevented from moving inboard by the strong energizing effect of the vortex field.

Figure 22(c) shows the flow field at a high angle of attack (16.7°), where extensive flow separation would be expected. However, the flow field has changed little from that for an angle of attack of 10.8°. The photograph reveals that the vortex flow has limited the spread of flow separation on the rear portion of the wing. That there is little change in the flow field from the moderate to the high angle of attack is generally confirmed by the flight data in that buffet intensity tends to level off at the higher angles of attack and in that there is no sharp break indicating extensive separation in the normal-force curves.

CONCLUDING REMARKS

Data from maneuvers performed during the first flight tests of the prototype YF-16 and YF-17 lightweight fighters were analyzed to assess the buffet and wing rock characteristics of the aircraft. Both aircraft were undergoing control system or flap deflection schedule modifications or both; therefore, the data presented do not necessarily represent the optimum configurations. The following conclusions were reached:

1. At subsonic speeds, the buffet intensity rise boundaries of the lightweight fighters are significantly higher than those of other current aircraft. At transonic speeds, the boundaries are comparable to or higher than those of similar low aspect ratio thin-winged aircraft.

2. For both aircraft, the combination of forebody strakes and scheduled flap deflections reduced the buffet intensities at high angles of attack. Significantly higher normal-force coefficients were obtainable in maneuvering flight than with most current aircraft.

3. A mild to moderate wing rock condition occurred on both aircraft over the Mach number range tested.

4. The buffet intensity rise boundaries can be raised to higher normal-force coefficients through improved flap deflection scheduling. The data showed that the wing rock boundary for the YF-17 airplane could be raised with improved flap deflection scheduling; comparable data were not available for the YF-16 airplane.

Dryden Flight Research Center
 National Aeronautics and Space Administration
  Edwards, Calif., October 21, 1976

REFERENCES

1. Fischel, Jack; and Friend, Edward L.: Preliminary Assessment of Effects of Wing Flaps on High Subsonic Flight Buffet Characteristics of Three Airplanes. NASA TM X-2011, 1970.

2. Friend, Edward L.; and Sefic, Walter J.: Flight Measurements of Buffet Characteristics of the F-104 Airplane for Selected Wing-Flap Deflections. NASA TN D-6943, 1972.

3. Friend, Edward L.; and Monaghan, Richard C.: Flight Measurements of Buffet Characteristics of the F-111A Variable-Sweep Airplane. NASA TM X-1876, 1969.

4. Monaghan, Richard C.; and Friend, Edward L.: Effects of Flaps on Buffet Characteristics and Wing-Rock Onset of an F-8C Airplane at Subsonic and Transonic Speeds. NASA TM X-2873, 1973.

5. Sisk, Thomas R.; Friend, Edward L.; Carr, Peter C.; and Sakamoto, Glenn M.: Use of Maneuver Flaps To Enhance the Transonic Maneuverability of Fighter Aircraft. NASA TM X-2844, 1973.

6. Ray, Edward J.; McKinney, Linwood W.; and Carmichael, Julian G.: Maneuver and Buffet Characteristics of Fighter Aircraft. NASA TN D-7131, 1973.

7. Sisk, Thomas R.; Kier, David A.; and Carr, Peter C.: Factors Affecting Tracking Precision of Fighter Aircraft. NASA TM X-2248, 1971.

8. Whitcomb, Richard T.: The NASA Supercritical Airfoil and Its Application to Swept Wings. Supercritical Wing Technology—A Progress Report on Flight Evaluations, NASA SP-301, 1972, pp. 1-11.

9. Ayers, Theodore G.; and Decker, John P.: Effects of Leading- and Trailing-Edge Flaps on the Aerodynamic Characteristics of a Thin Cranked-Wing Model at Mach Numbers From 0.20 to 1.20. NASA TM X-2098, 1970.

10. Mechtly, E. A.: The International System of Units—Physical Constants and Conversion Factors. Second Revision. NASA SP-7012, 1973.

11. Kaiser, J. F.: Digital Filters. Ch. 7 of System Analysis by Digital Computer, Franklin F. Kuo and James F. Kaiser, eds., John Wiley & Sons, Inc., c.1966, pp. 218-285.

12. Graham, Dustan; and Lathrop, R. C.: The Synthesis of "Optimum" Transient Response: Criteria and Standard Forms. AIEE Transactions, Vol. 72. Part II, Applications and Industry, Nov. 1953, pp. 273-288.

13. Warren, Michael Edward: Ride Comfort Control in Large Flexible Aircraft. NASA CR-116775, 1971.

14. Sisk, Thomas R.: A Preliminary Assessment of the Transonic Maneuvering Characteristics of Two Advanced Technology Fighter Aircraft. NASA TM X-3439, 1976.

15. Mabey, D. G.: Beyond the buffet boundary. Aeron. J., vol. 77, no. 748, Apr. 1973, pp. 201-215.

TABLE 1.- PHYSICAL CHARACTERISTICS OF TEST AIRCRAFT WINGS

	YF-16	YF-17	F-5A
Wing			
Airfoil section	NACA 64A204 (modified)	NACA 65A (modified)	NACA 65A004.8 (modified)
Span, m (ft)[a]	8.83 (29)	10.67 (35.0)	7.68 (25.25)
Area, m^2 (ft^2).	26.0 (280)	32.5 (350)	16.22 (174)
Leading-edge sweep, deg	40	26	32
Aspect ratio	3.00	3.50	3.75
Taper ratio	0.20	0.35	0.20
Camber, percent mean aerodynamic chord.	2	1	0.7
Thickness-to-chord ratio.	0.04	0.05/0.04[b]	0.048
Leading-edge flap			
Type	Plain	Plain	Plain
Area (both), m^2 (ft^2)	3.07 (33.03)	4.27 (46)	1.14 (12.3)
Chord, percent mean aerodynamic chord.	20	20	15
Span, percent semispan	69	75	58
Maximum flap deflection perpendicular to hinge line, deg . . .	25	24	23 (root), 18 (tip)[c]
Trailing-edge flap			
Type	Plain	Plain	Plain
Area (both), m^2 (ft^2)	2.58 (27.72)	4.74 (51)	1.78 (19.0)
Chord, percent mean aerodynamic chord.	20	30	26.1
Span, percent semispan	61	46	30
Maximum flap deflection perpendicular to hinge line, deg . . .	20	20	20

[a]Not including missiles or launcher rails.

[b]25-percent semispan/65-percent semispan.

[c]Design twist of 5 percent (23° root and 18° tip) removed by insertion of machined blocks for partial deflections of fixed flap program (ref. 5).

TABLE 2.—TEST FLAP DEFLECTION MATRIX
[Values of Mach number and flap deflection are nominal]

(a) YF-16 airplane

M	δ_{le}, deg	δ_{te}, deg
0.80	0 5 10 15 25 Scheduled Scheduled	0 0 0 0 0 8 16
0.85	0 5 10 15 25 Scheduled Scheduled Scheduled	0 0 0 0 0 8 16 20
0.95	0 5 10 15 25	0 0 0 0 0

(b) YF-17 airplane

M	δ_{le}, deg	δ_{te}, deg
0.80	0 3 6 10 12 6 8 10 11	5 to 7 5 to 7 5 to 7 5 to 7 5 to 7 12 to 15 12 to 15 12 to 15 12 to 15
0.90	0 4 5 10 0 4 6 8 10 4 5 8	0 0 0 0 5 to 7 5 to 7 5 to 7 5 to 7 5 to 7 10 10 10

Figure 1. Lightweight fighter prototypes.
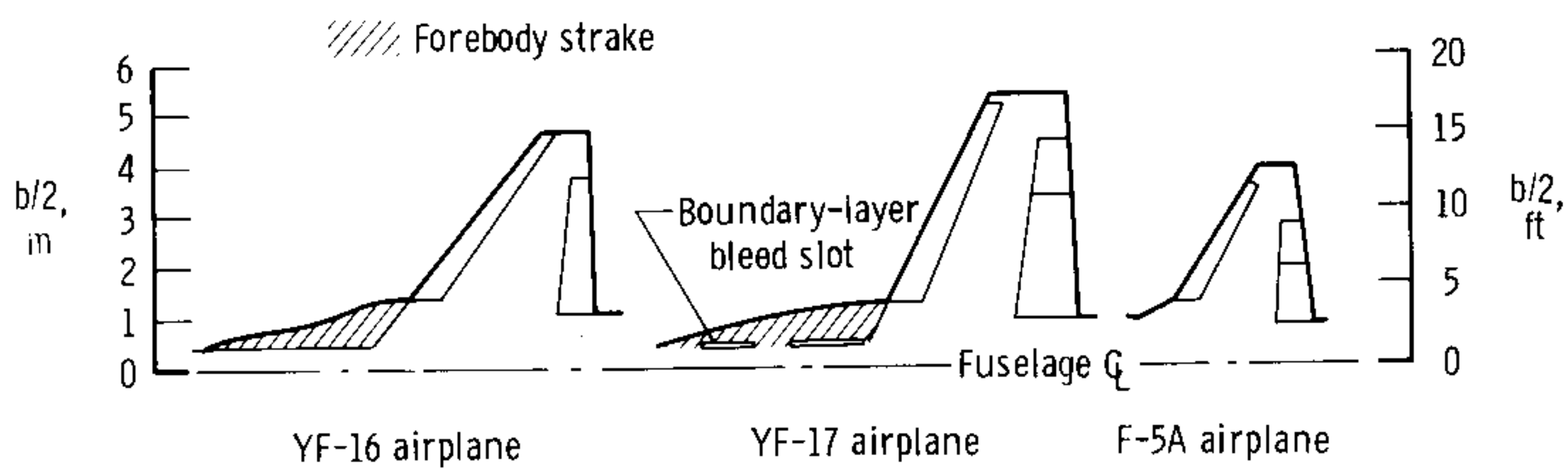
Figure 2. Wing planforms.
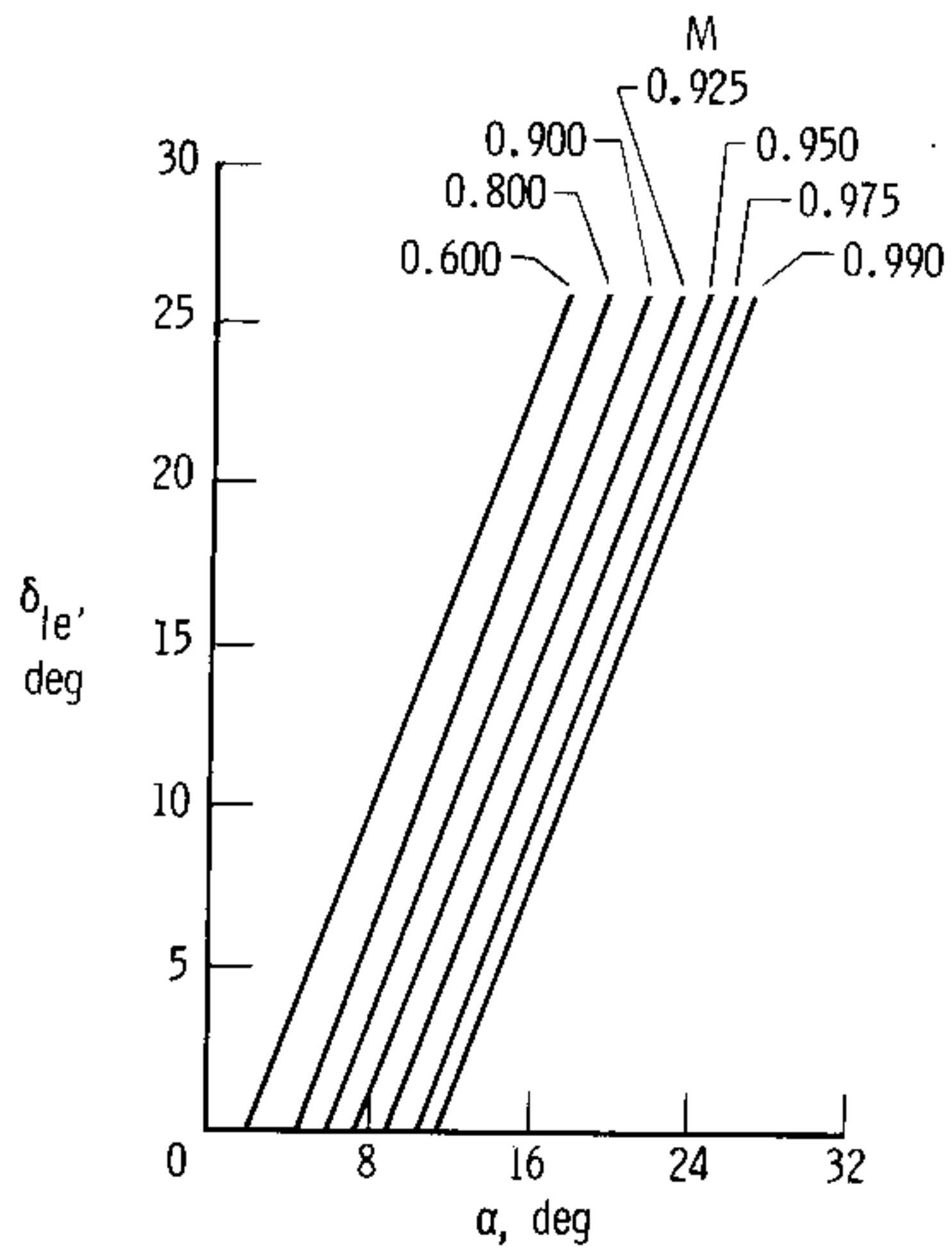
(a) YF-16 airplane.
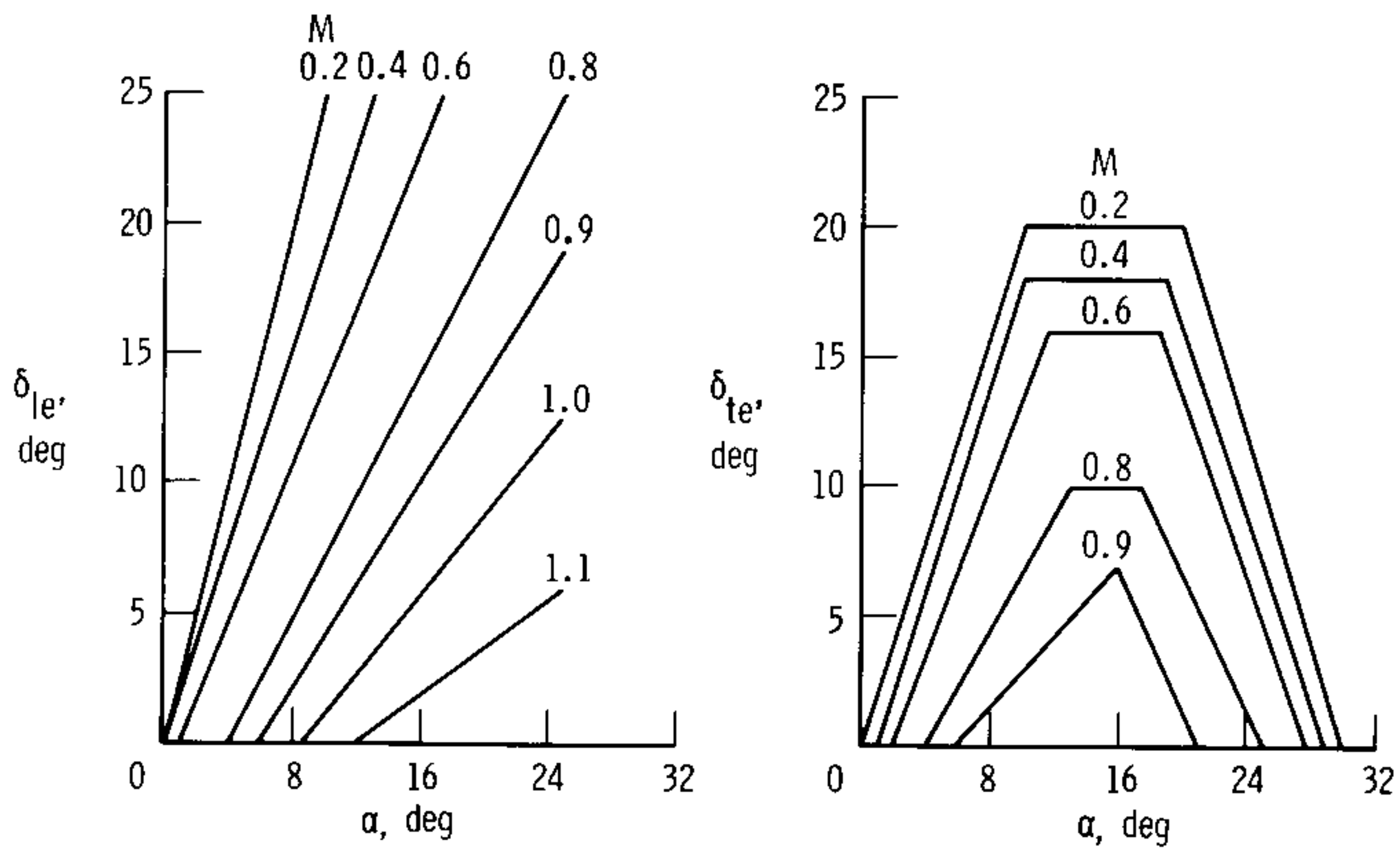
(b) YF-17 airplane.

Figure 3. Flap deflection schedules.
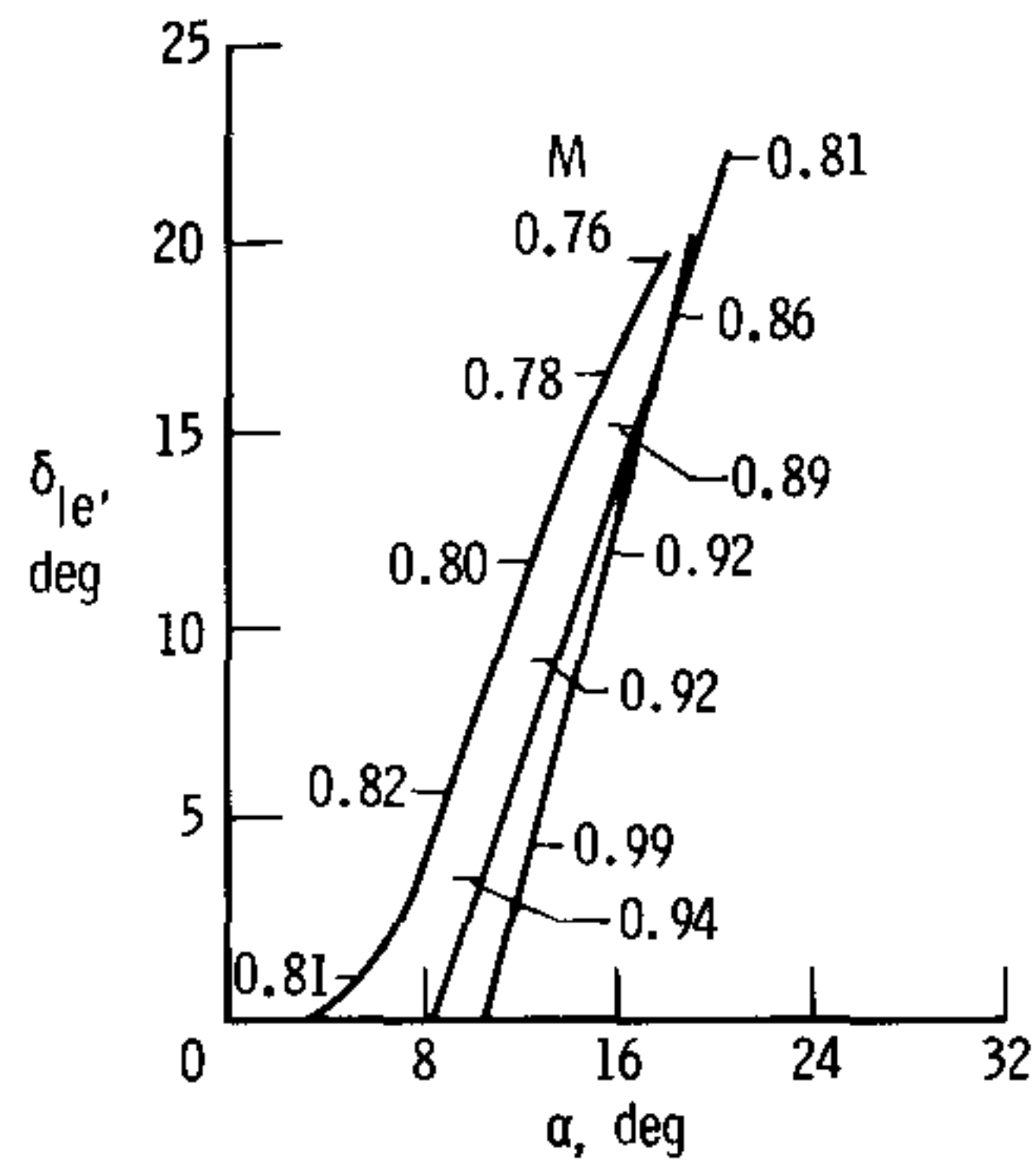
(a) YF-16 airplane.
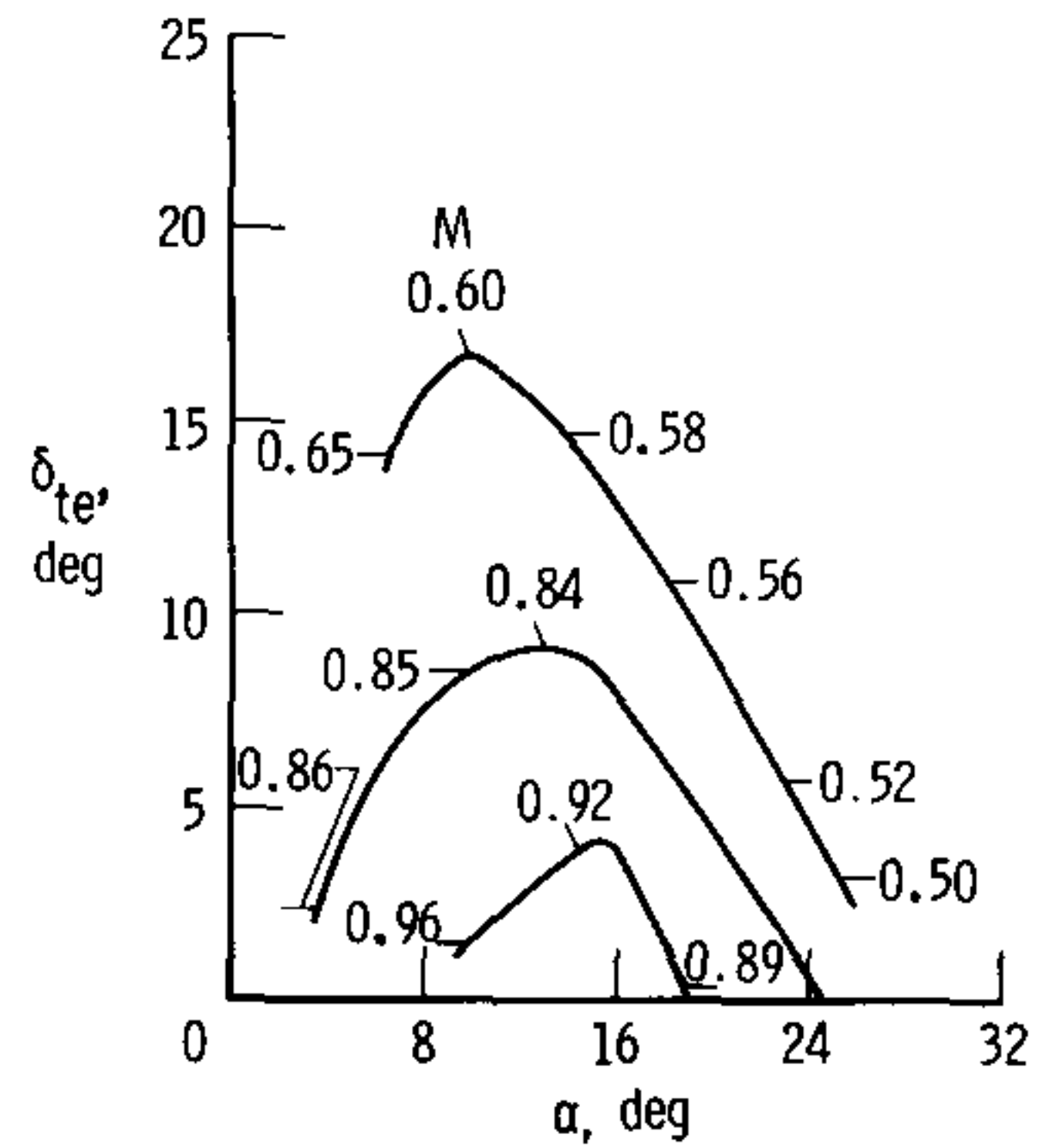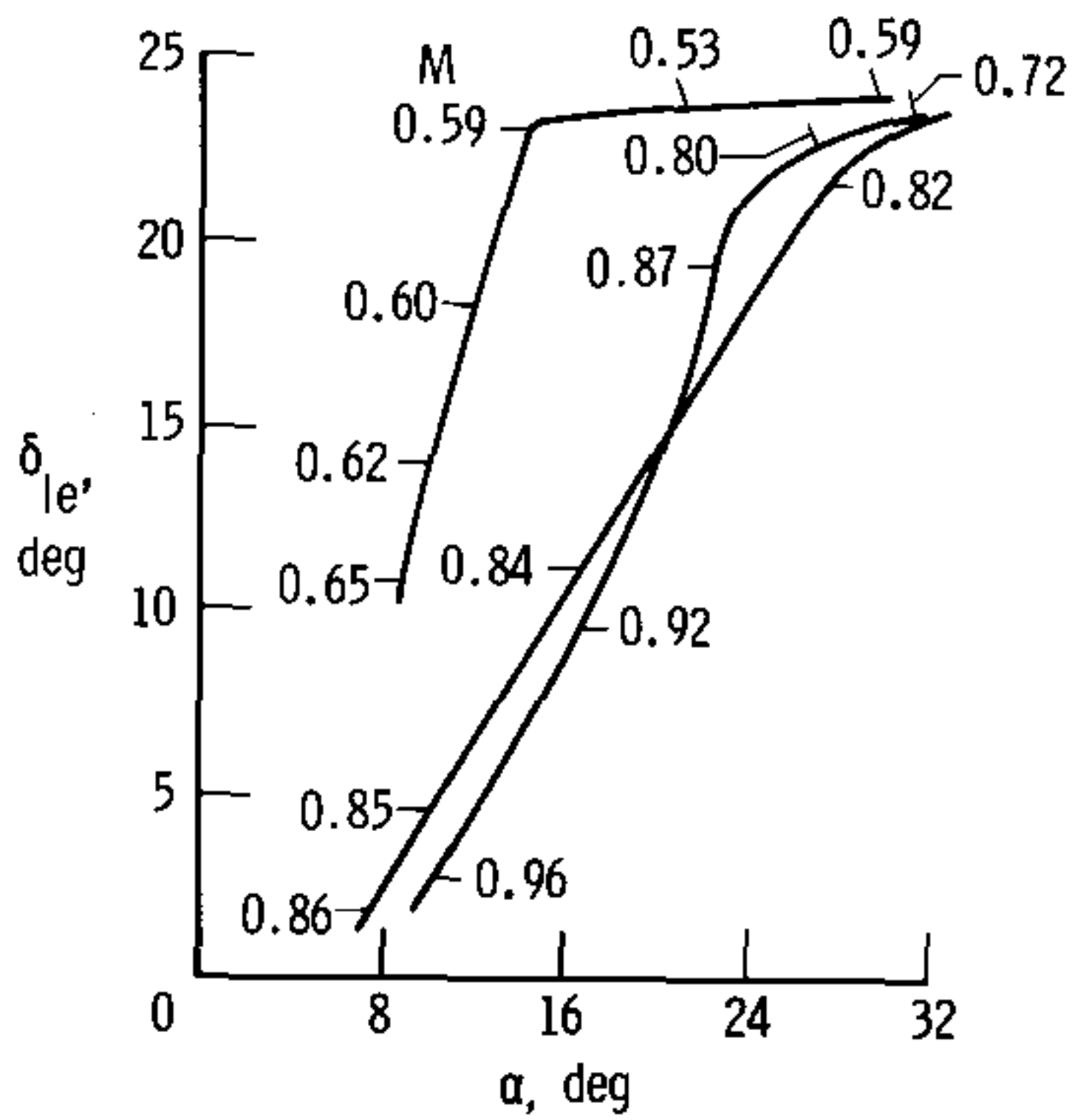
(b) YF-17 airplane.

Figure 4. Flap deflections measured in flight.

t, sec	M
0	0.94
2	0.94
4	0.94
6	0.93
8	0.93
10	0.92
12	0.90
14	0.89
16	0.90
18	0.90
20	0.87

α, deg — 20, 15, 10, 5, 0

β, deg — 2, 0, -2

p, deg/sec — 10, 0, -10, -20 — Wing rock onset

r, deg/sec — 5, 0, -5

F_Y, N — 20, 0, -20 ; F_Y, lb — 4, 0, -4

δ_a, deg — 5, 0, -5

δ_{a_h}, deg — 5, 0, -5

δ_r, deg — 2, 0, -2

δ_{le}, deg — 20, 10, 0

σ_{B_m}, (m-N) — 4×10^3, 3, 2, 1 — Buffet intensity rise ; σ_{B_m}, in-lb — 3×10^4, 2, 1, 0

t, sec — 0, 2, 4, 6, 8, 10, 12, 14, 16, 18, 20
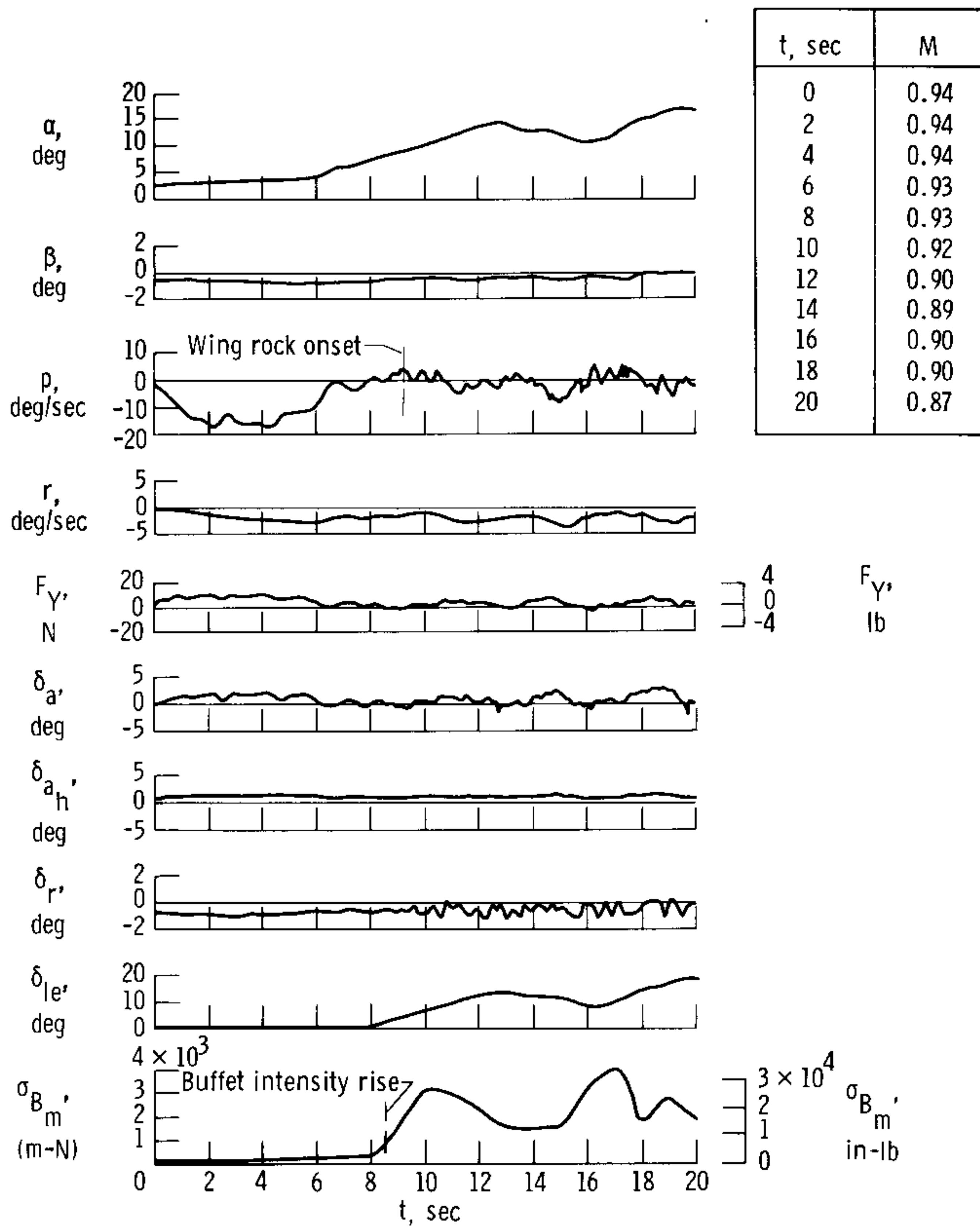
(a) Scheduled leading-edge flaps.

Figure 5. Time histories of YF-16 windup-turn maneuvers.

t, sec	M
0	0.87
2	0.87
4	0.87
6	0.81
8	0.87
10	0.88
12	0.90
14	0.88
16	0.87
18	0.86
20	0.84
22	----
24	0.79
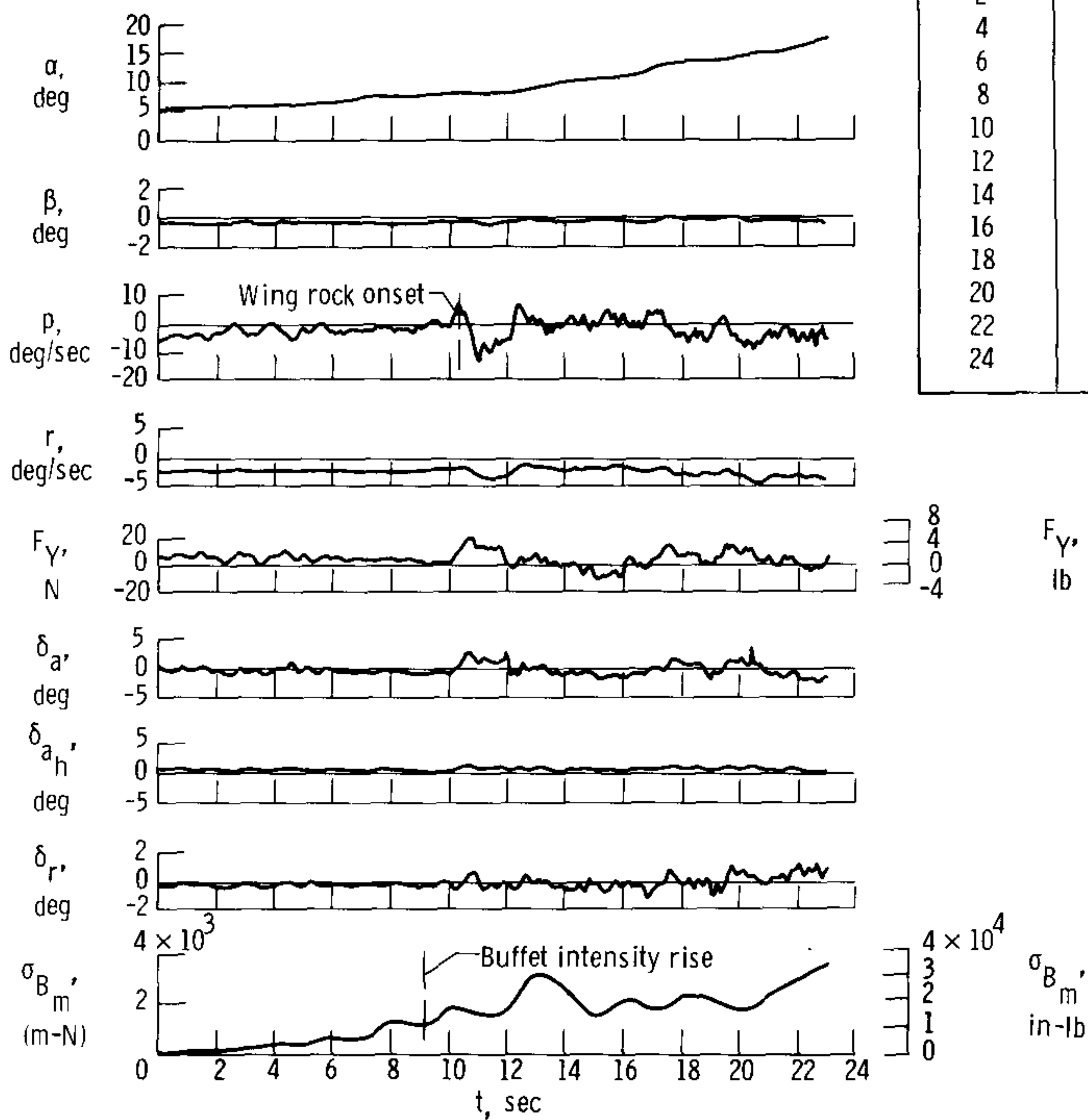
(b) Clean configuration.

Figure 5. Concluded.
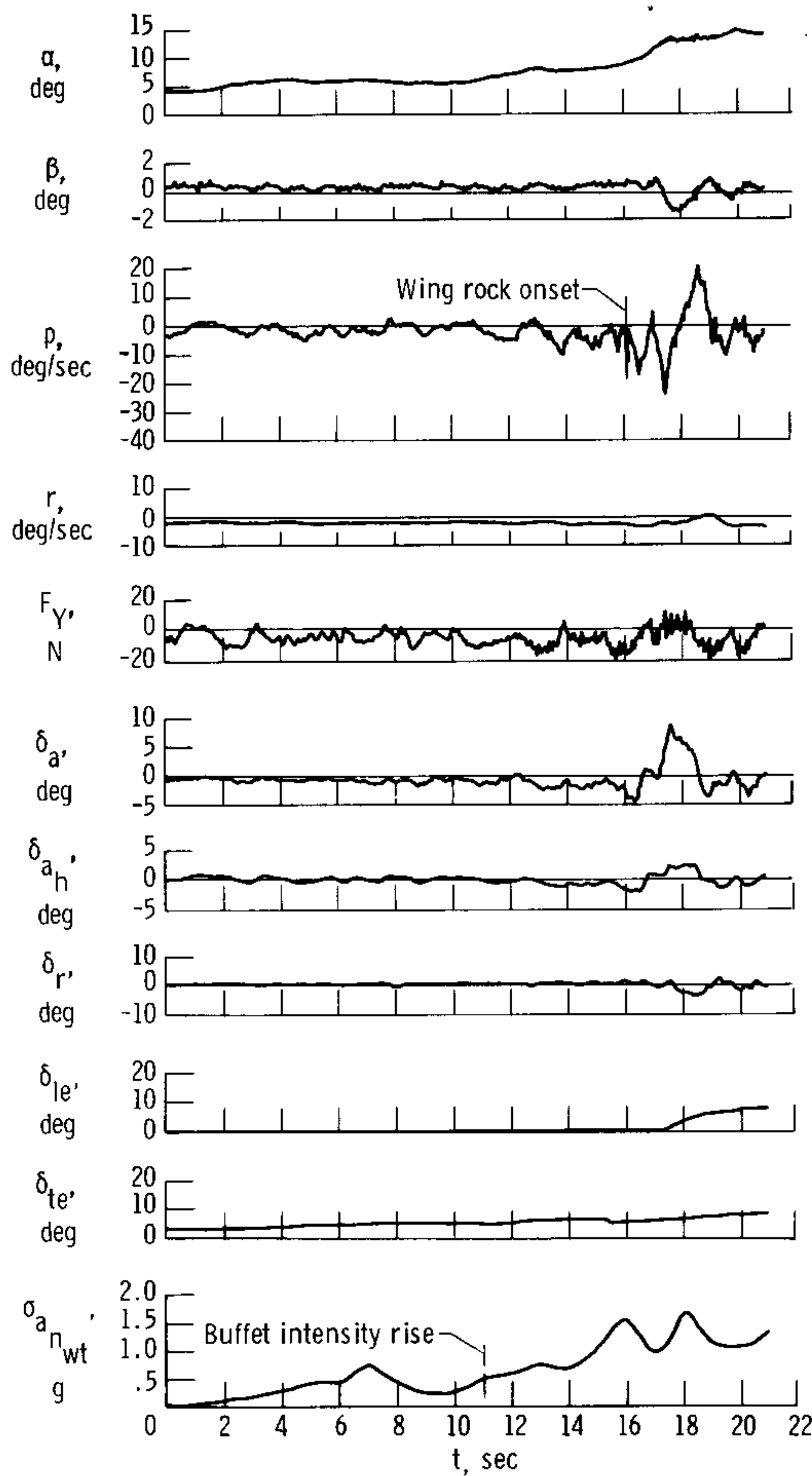
t, sec	M
0	0.90
2	0.91
4	0.90
6	0.90
8	0.90
10	0.91
12	0.91
14	0.91
16	0.90
18	0.87
20	0.85
22	----

(a) Scheduled flaps.

Figure 6. Time histories of YF-17 windup-turn maneuvers.

t, sec	M
0	0.90
2	0.90
4	0.90
6	0.90
8	0.89
10	0.89
12	0.91
14	0.91
16	0.91
18	0.88
20	0.83
22	0.81
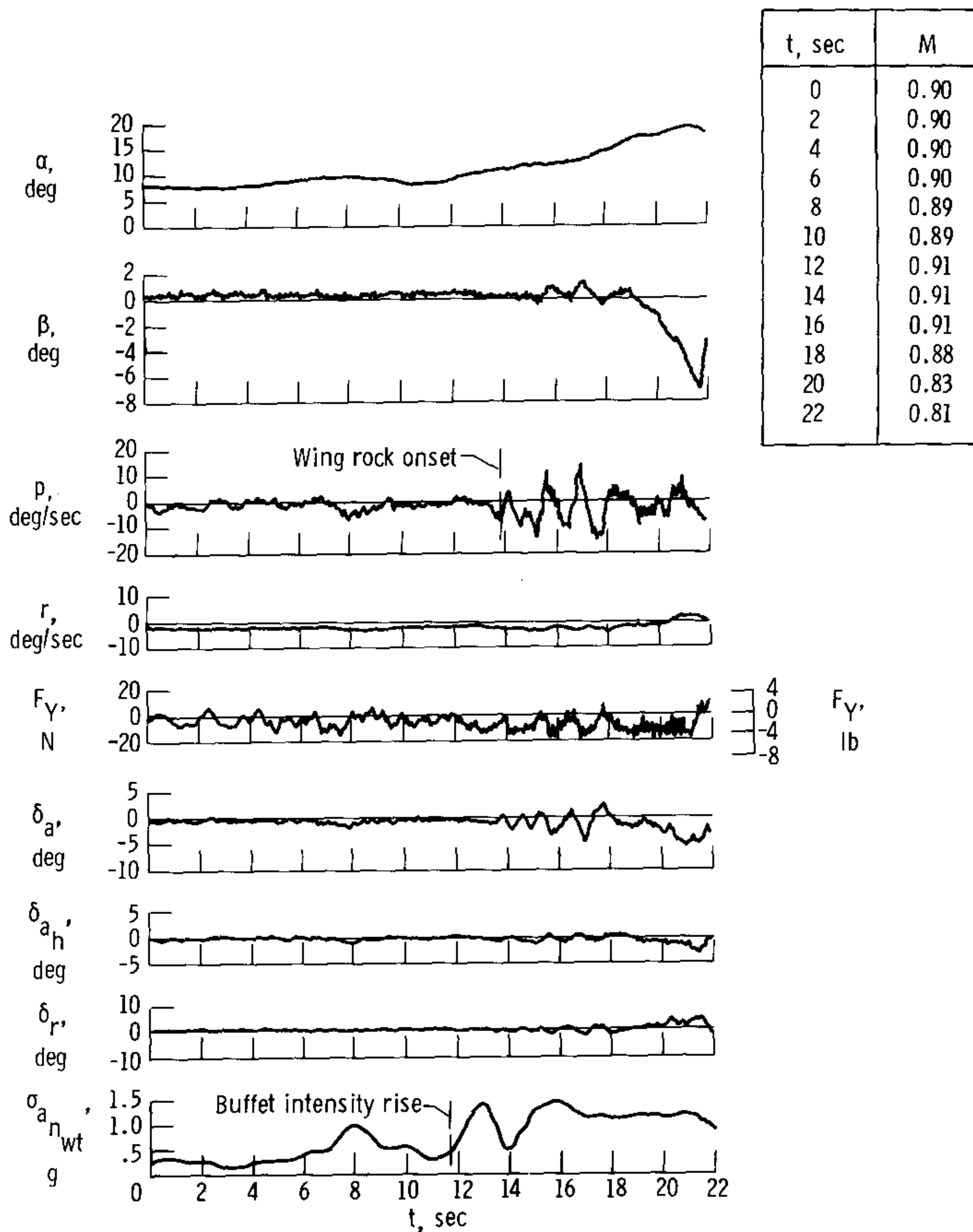
(b) Clean configuration.

Figure 6. Concluded.
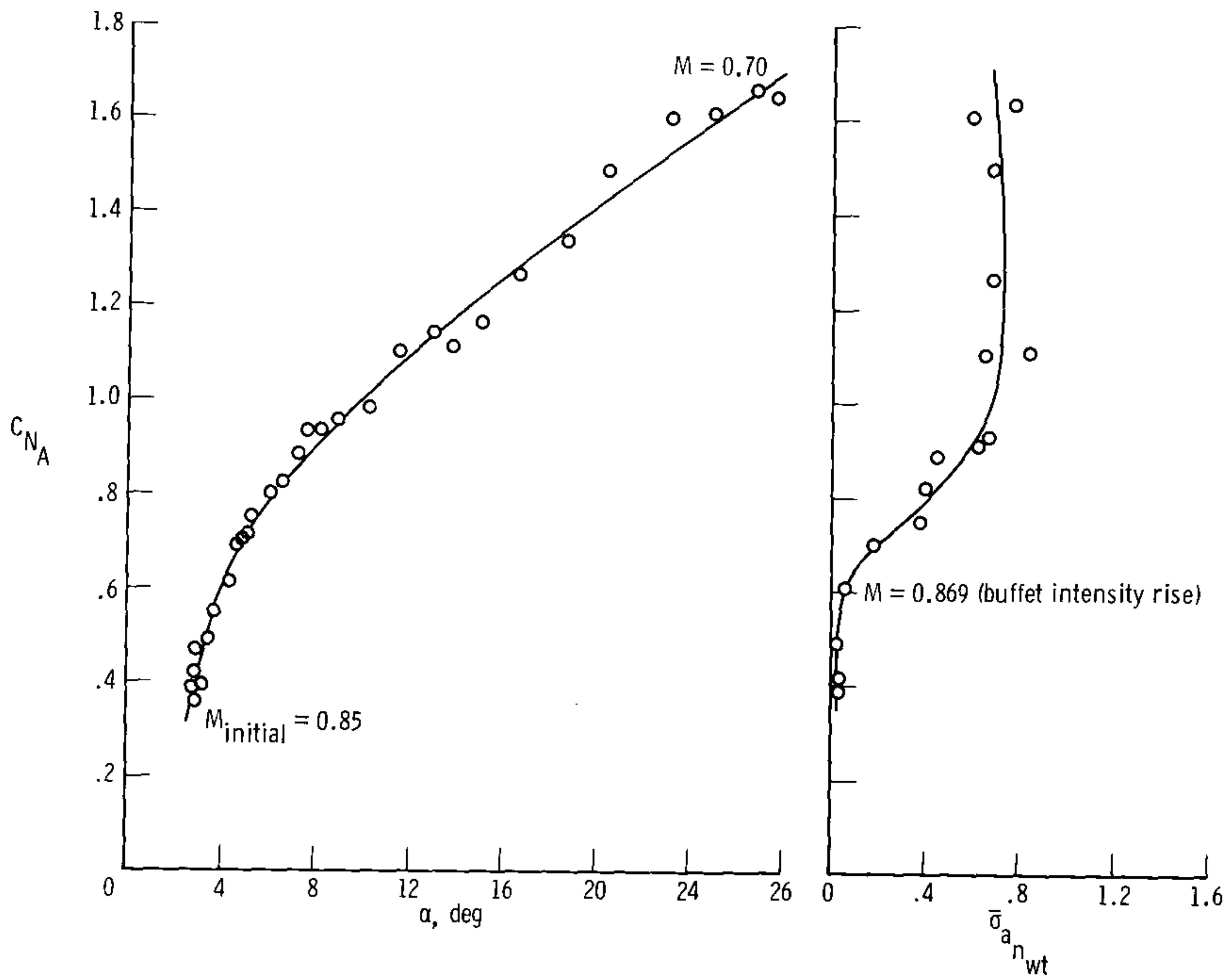
*Figure 7. Typical normal-force and buffet intensity characteristics.
YF-17 airplane.*
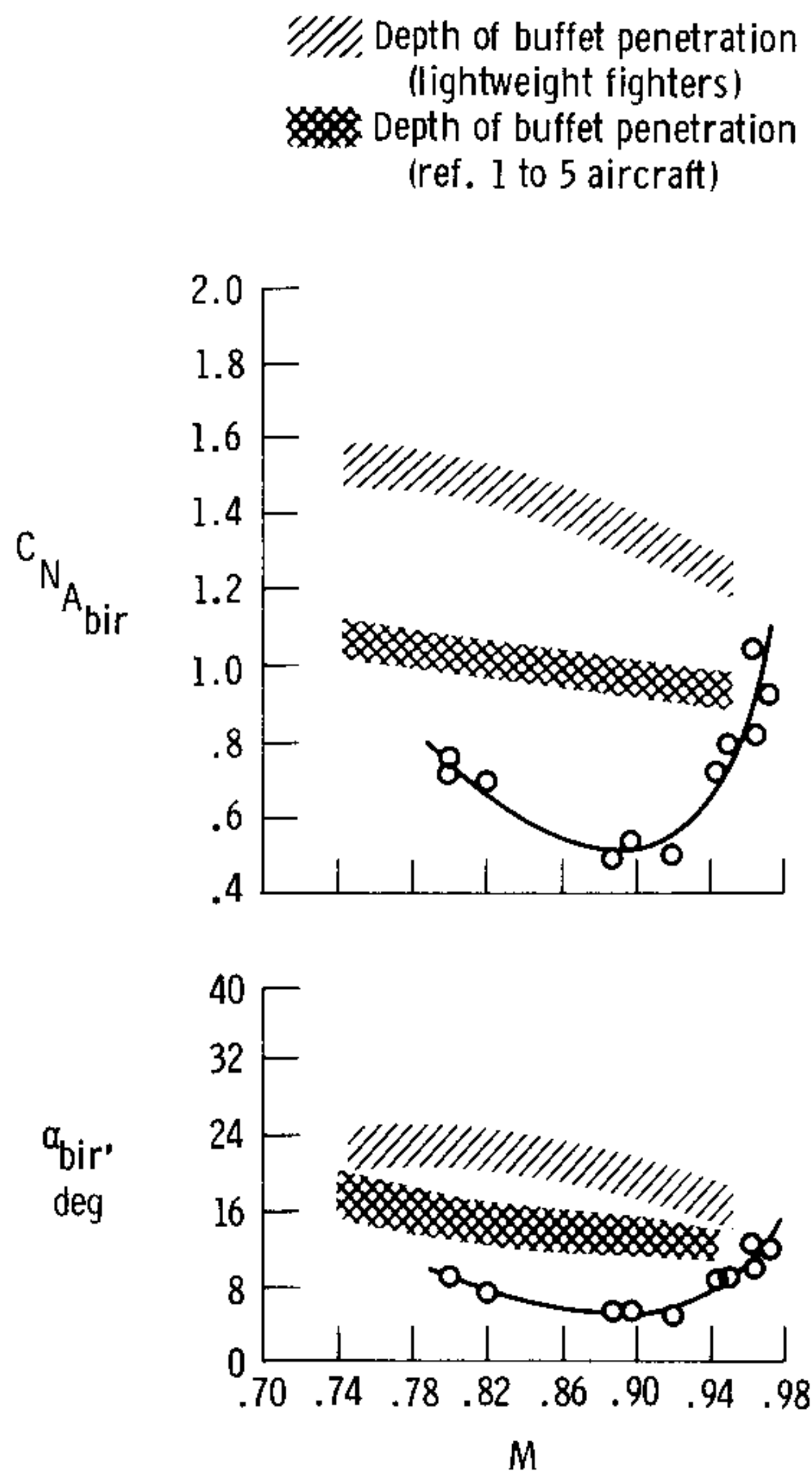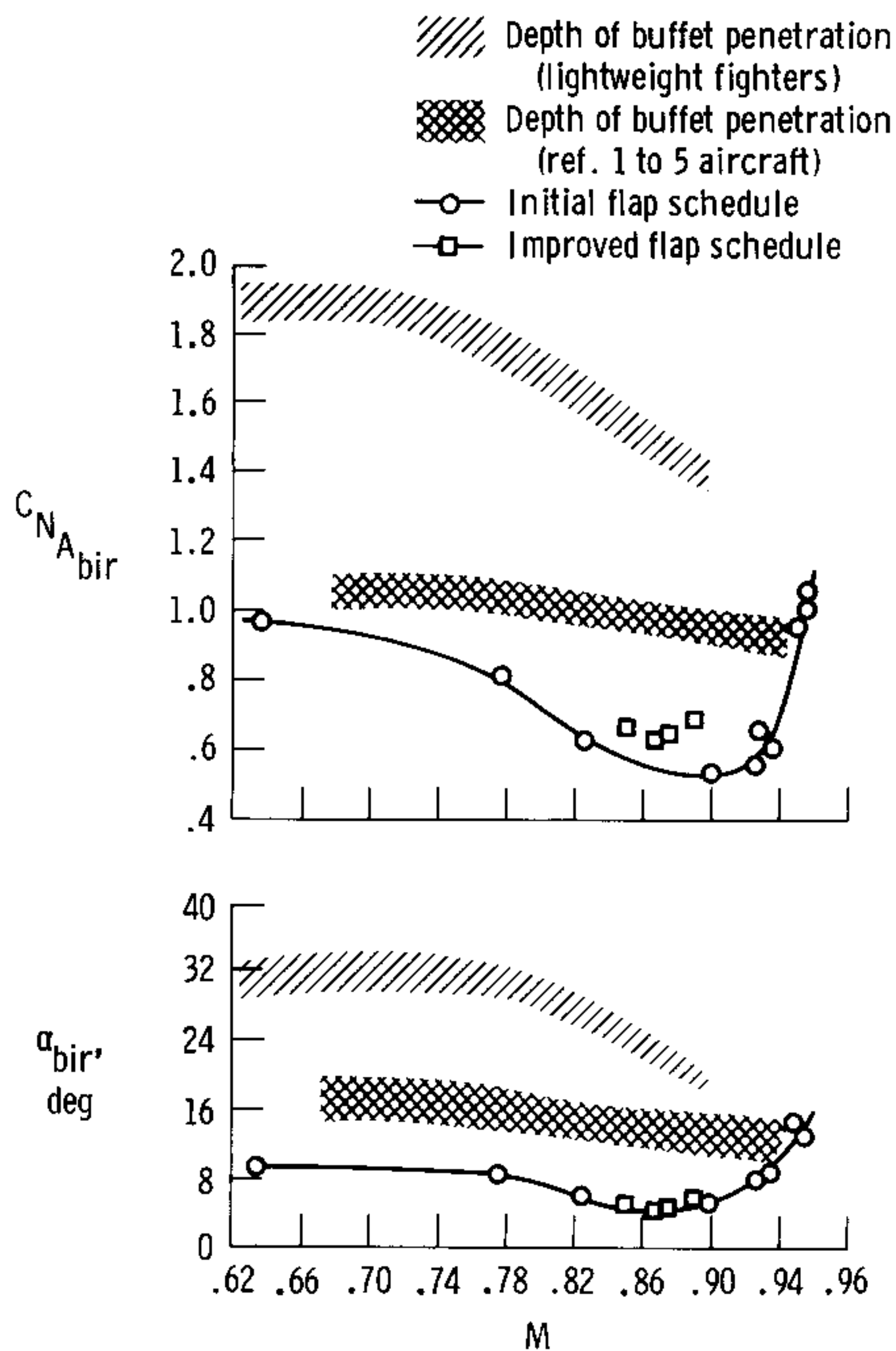
Figure 8. Variation of airplane normal-force coefficient and angle of attack for buffet intensity rise with Mach number.

(a) *YF-16 airplane.*   (b) *YF-17 airplane.*
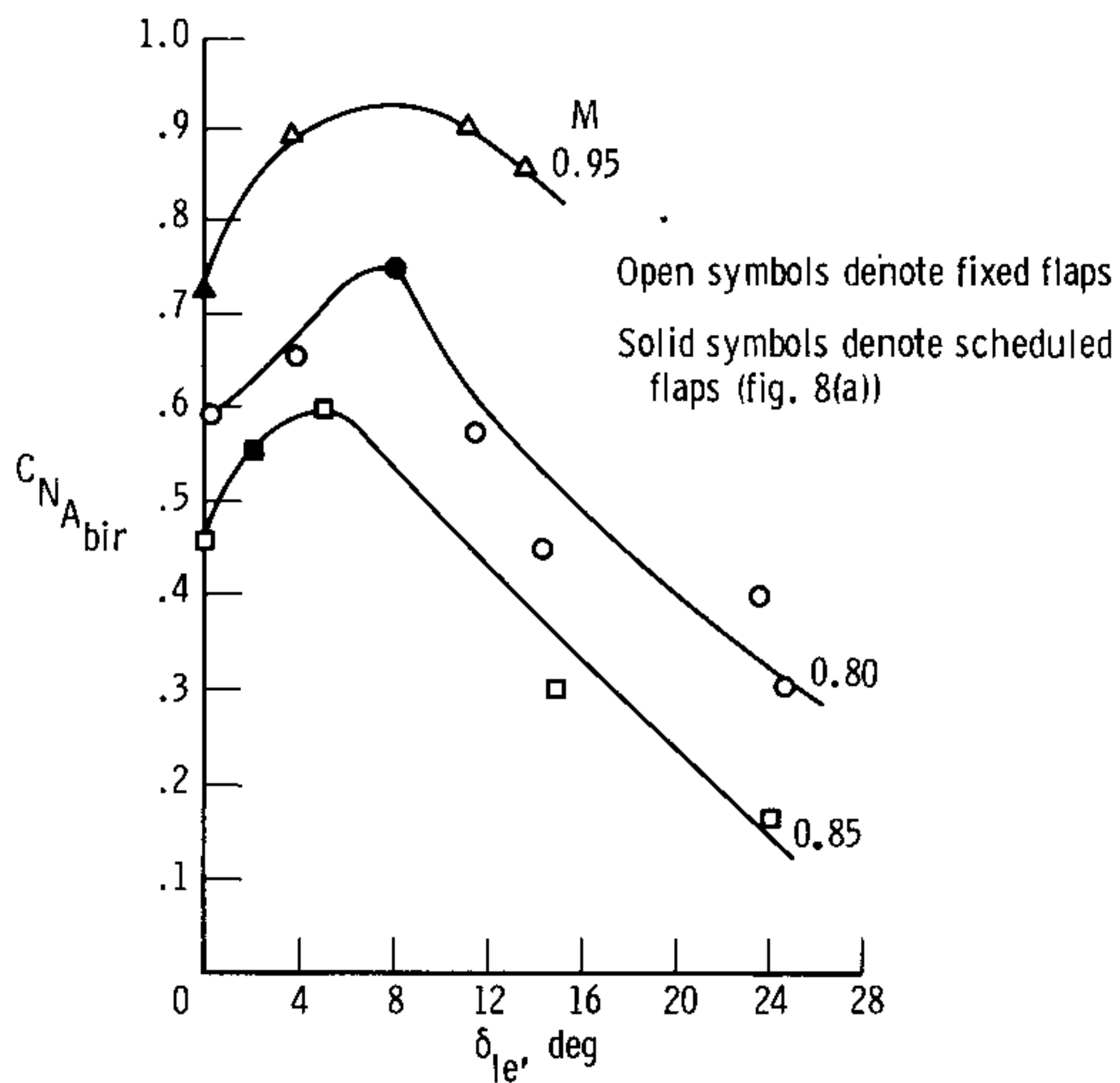
(a) $\delta_{te} = 0°$.
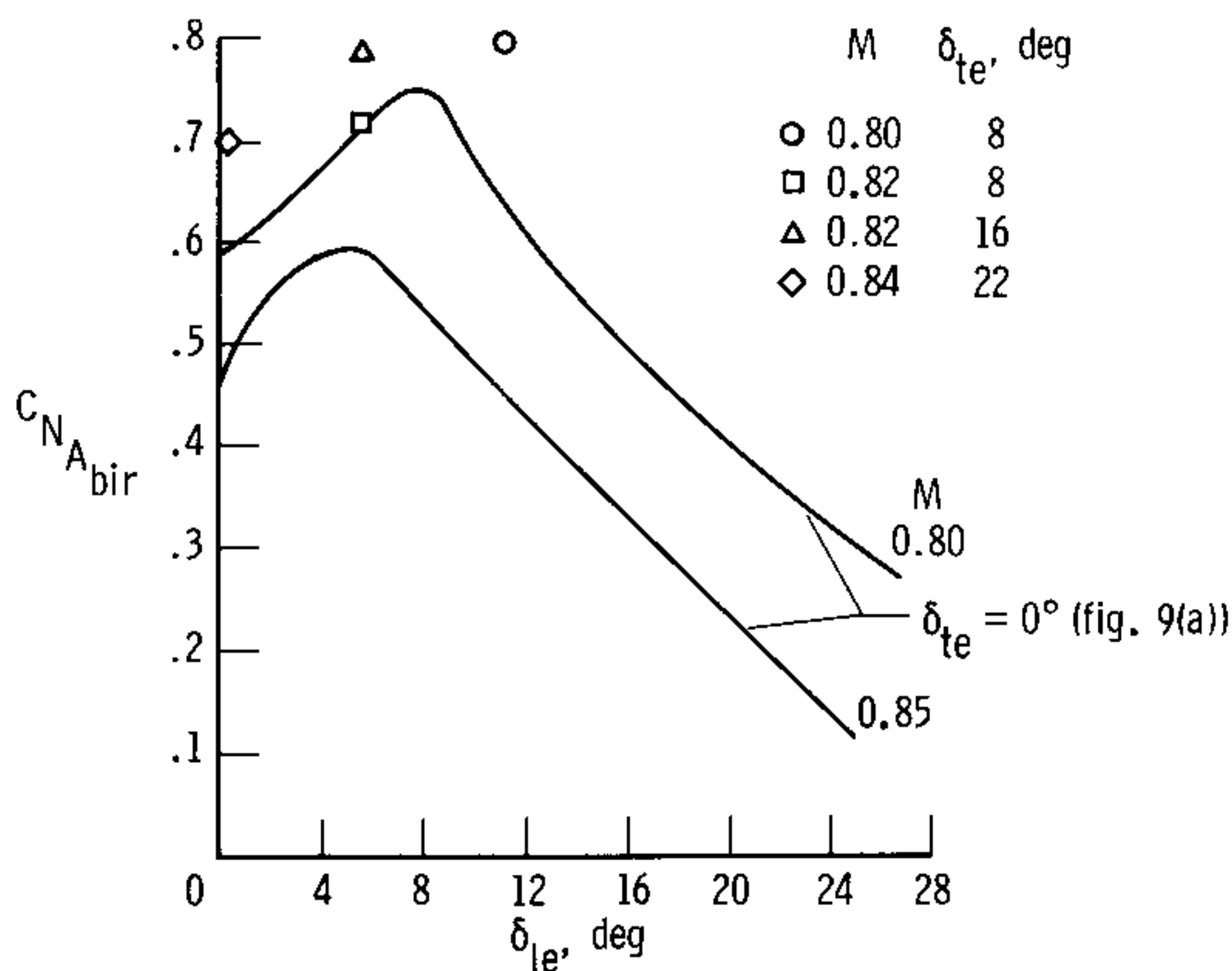
(b) Scheduled leading-edge flaps, fixed trailing-edge flaps (except for fairings).

Figure 9. YF-16 buffet intensity rise for fixed leading-edge flaps only and for scheduled leading-edge flaps in combination with fixed trailing-edge flaps.
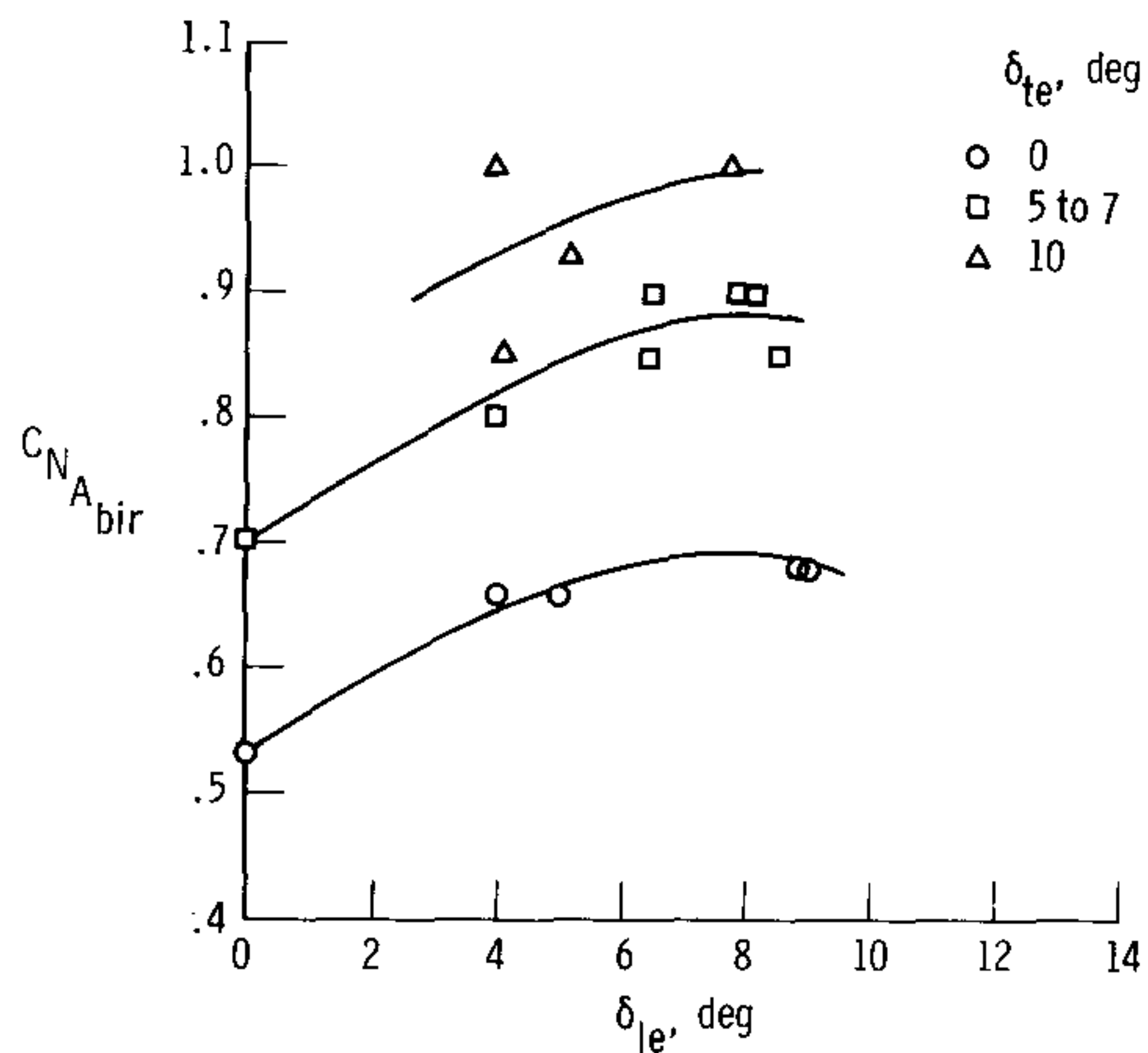
(a) Mach 0.90.
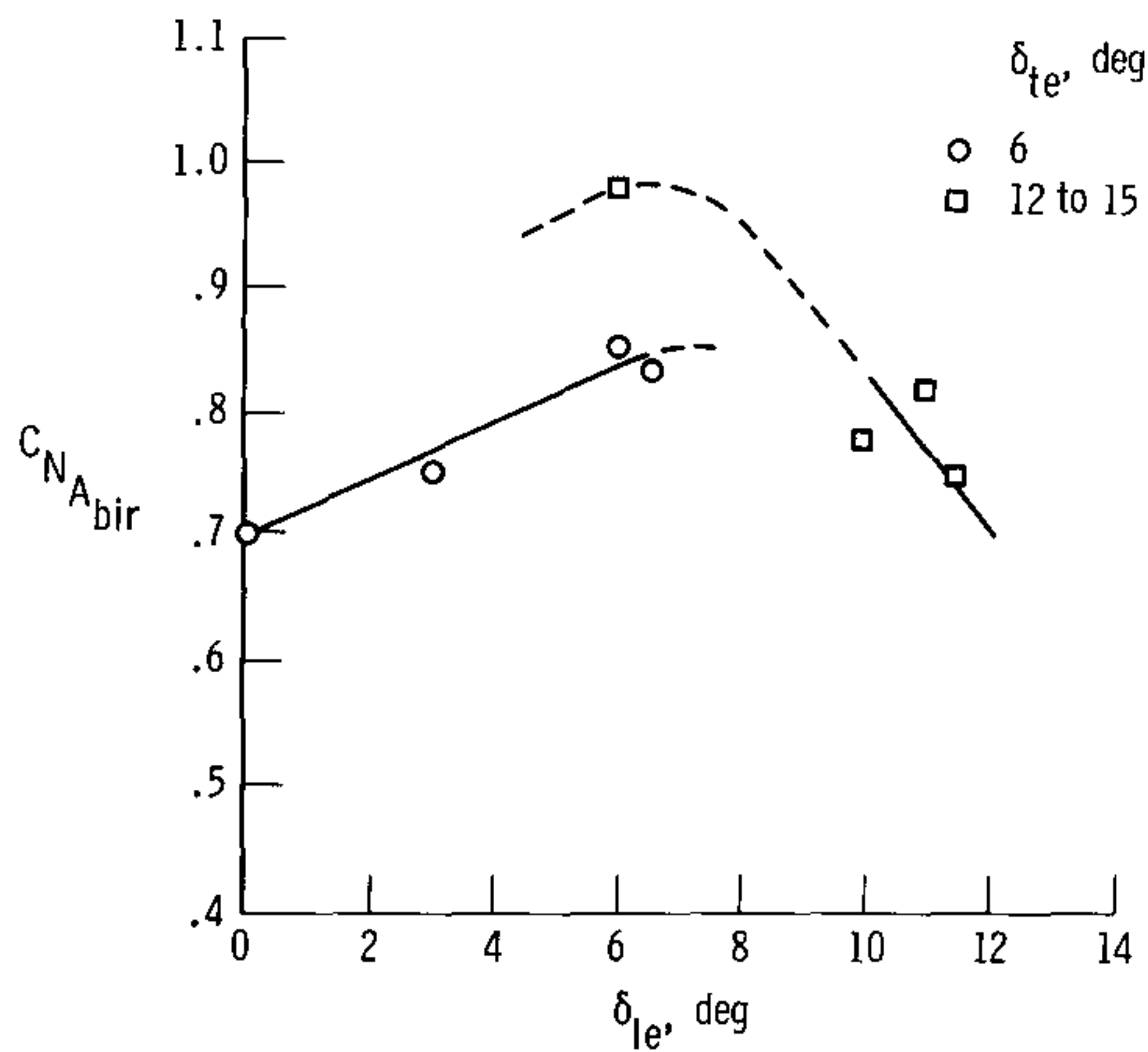
(b) Mach 0.80.

Figure 10. YF-17 buffet intensity rise for fixed leading-
and trailing-edge flaps.
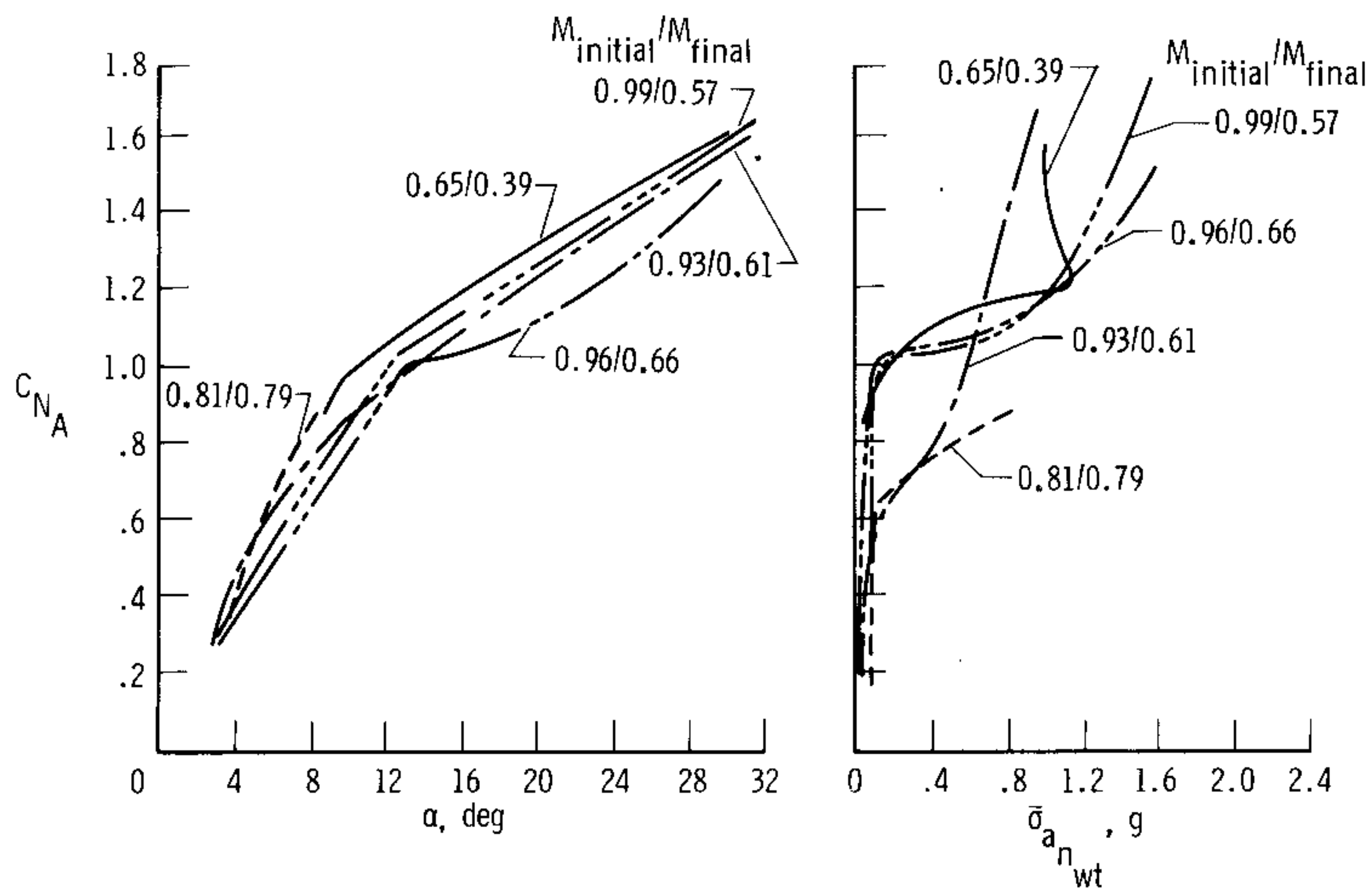
(a) YF-17 airplane.
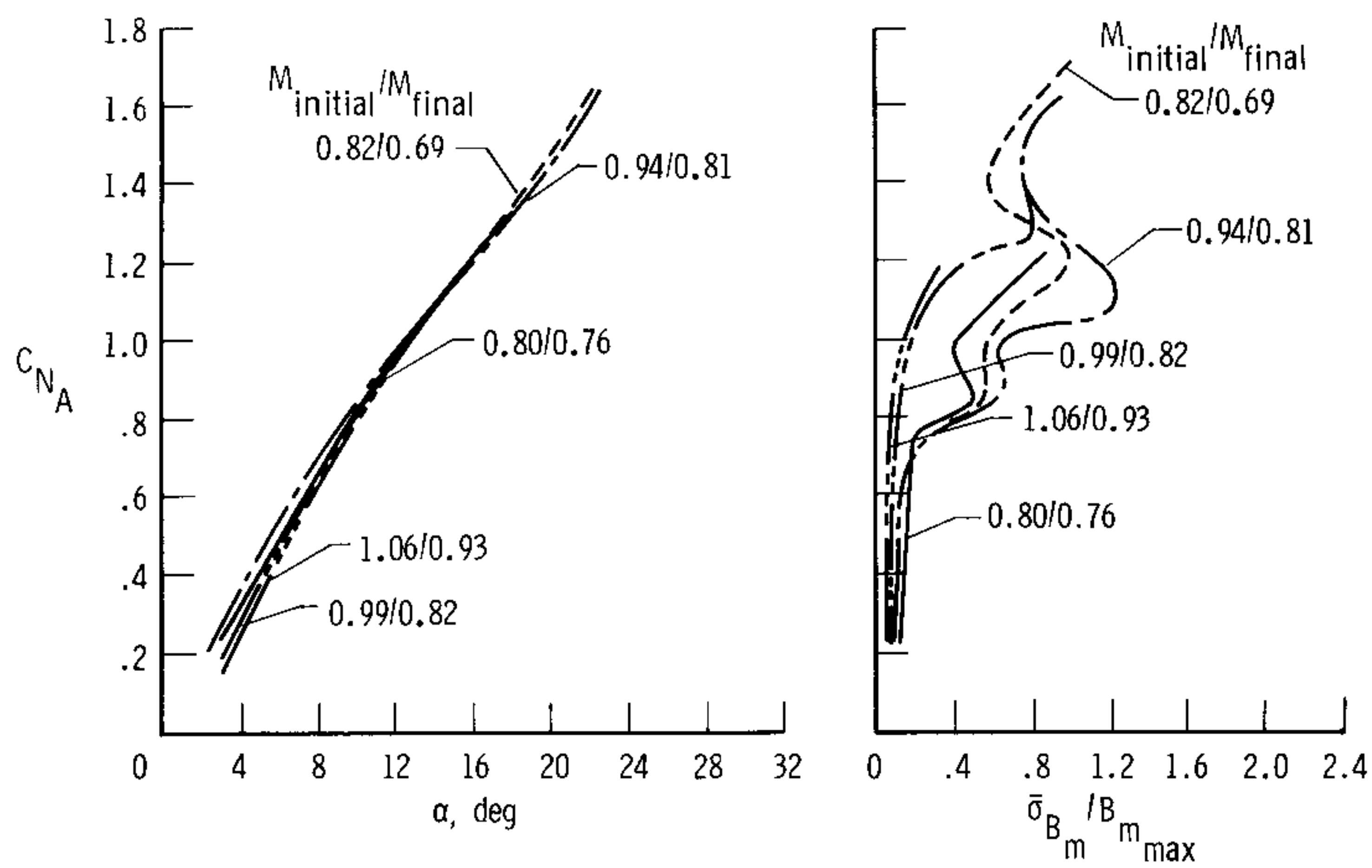
(b) YF-16 airplane.

Figure 11. Variation of airplane normal-force coefficients with angle of attack and buffet intensity at various Mach numbers for scheduled flaps.
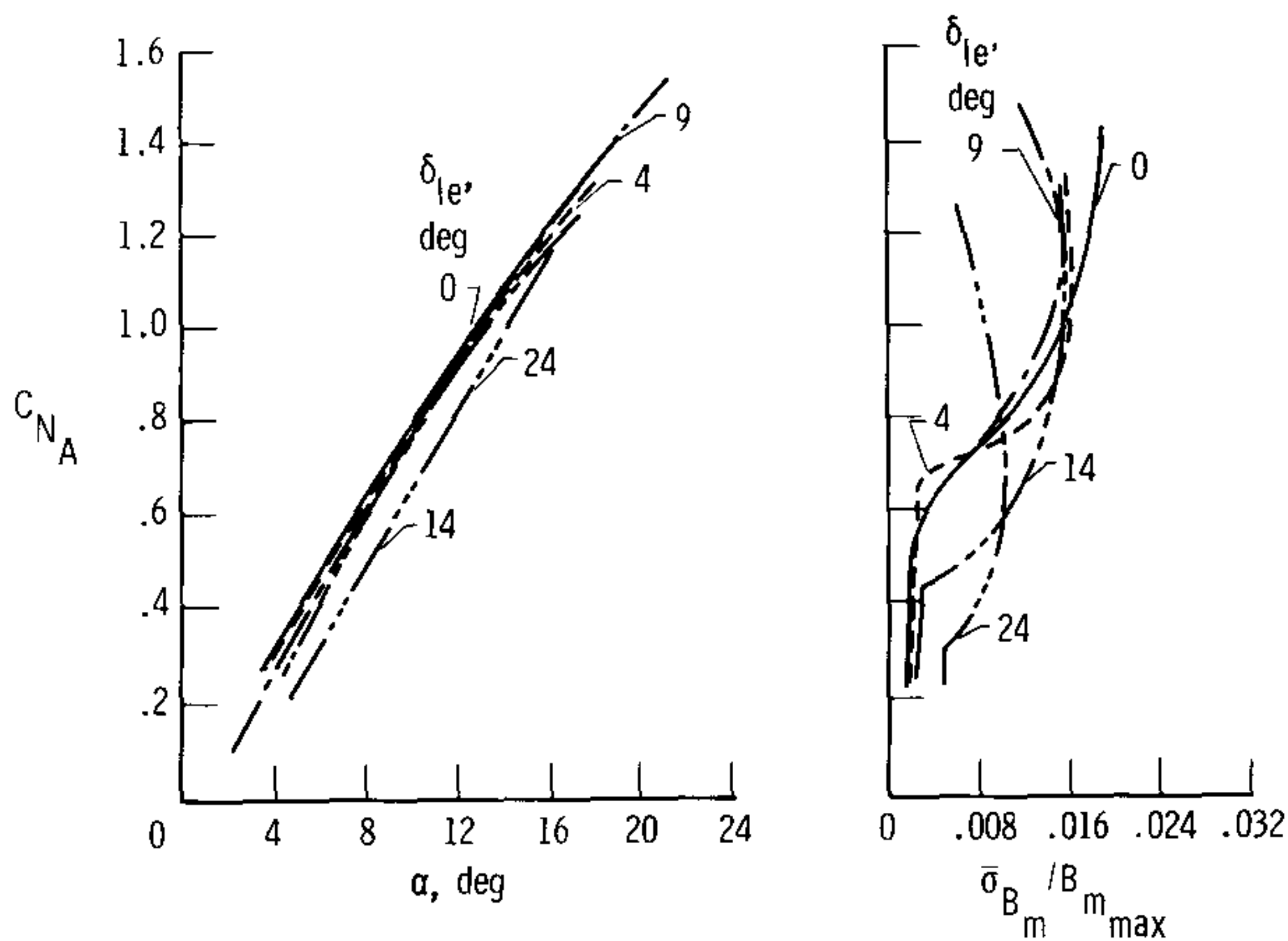
(a) Mach 0.80, fixed leading-edge flaps, $\delta_{te} = 0°$.
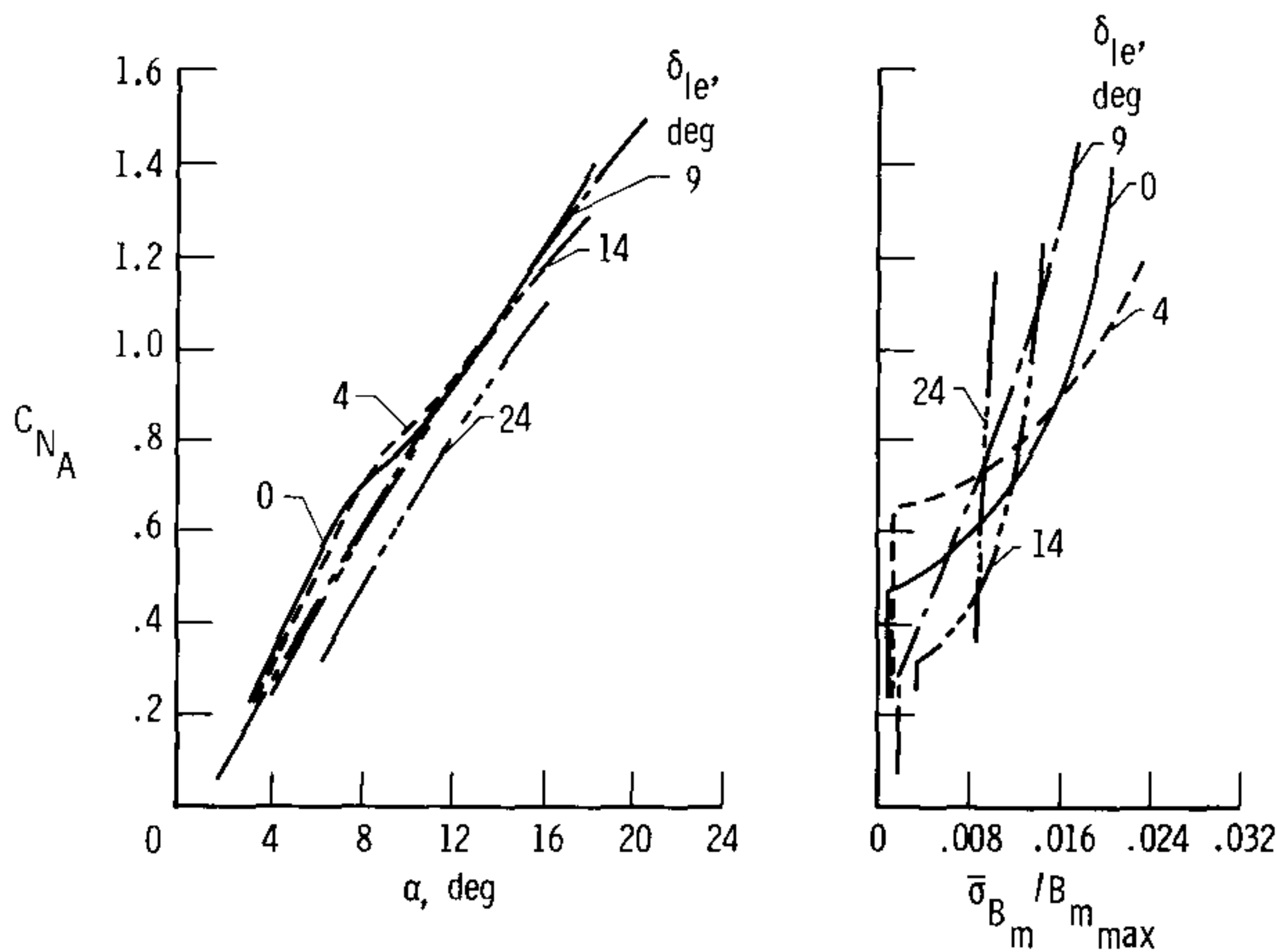
(b) Mach 0.85, fixed leading-edge flaps, $\delta_{te} = 0°$.

Figure 12. Variation of YF-16 normal-force coefficients with angle of attack and buffet intensity for various flap deflections.
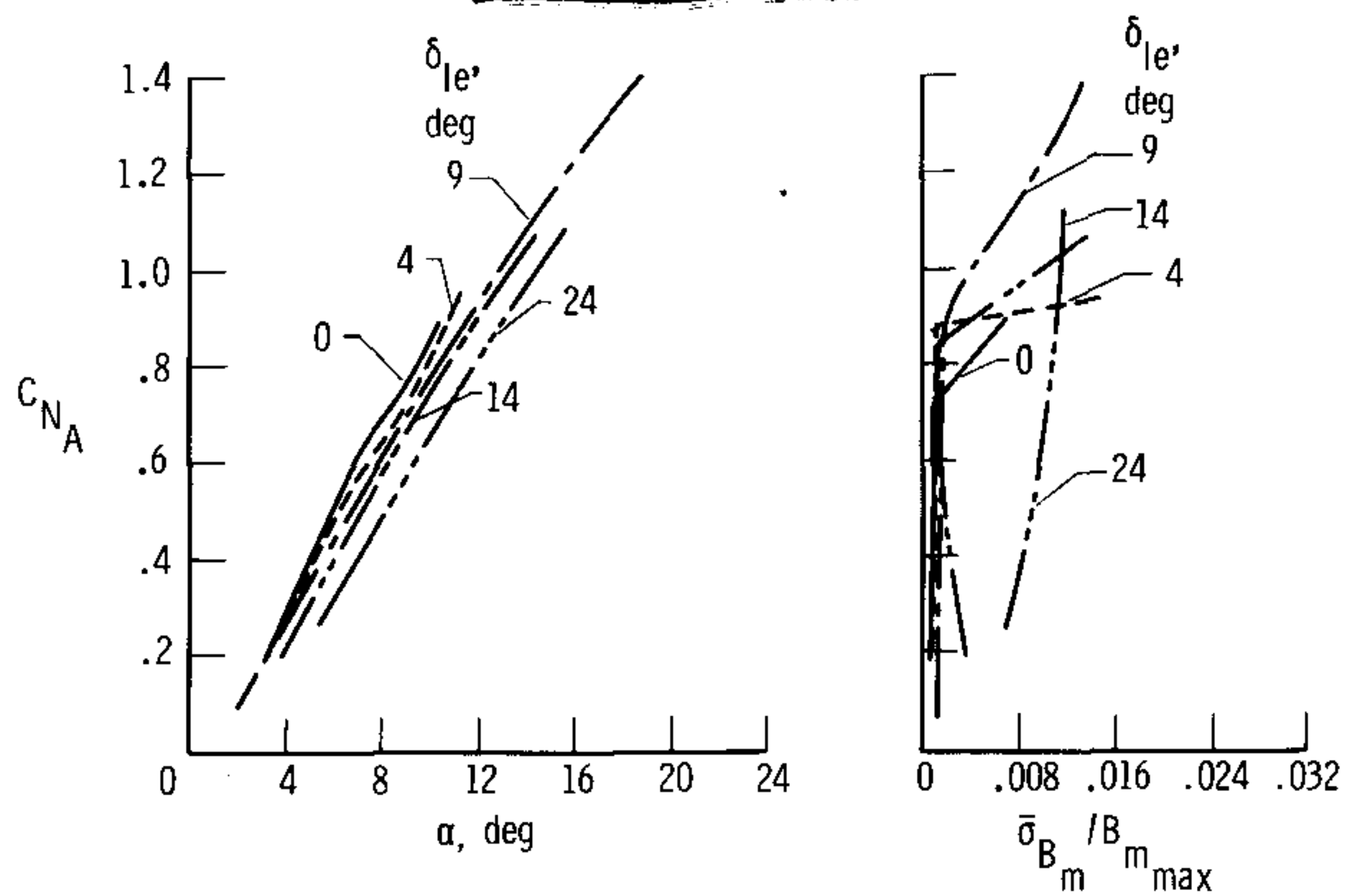
(c) Mach 0.95, fixed leading-edge flaps, $\delta_{te} = 0°$.
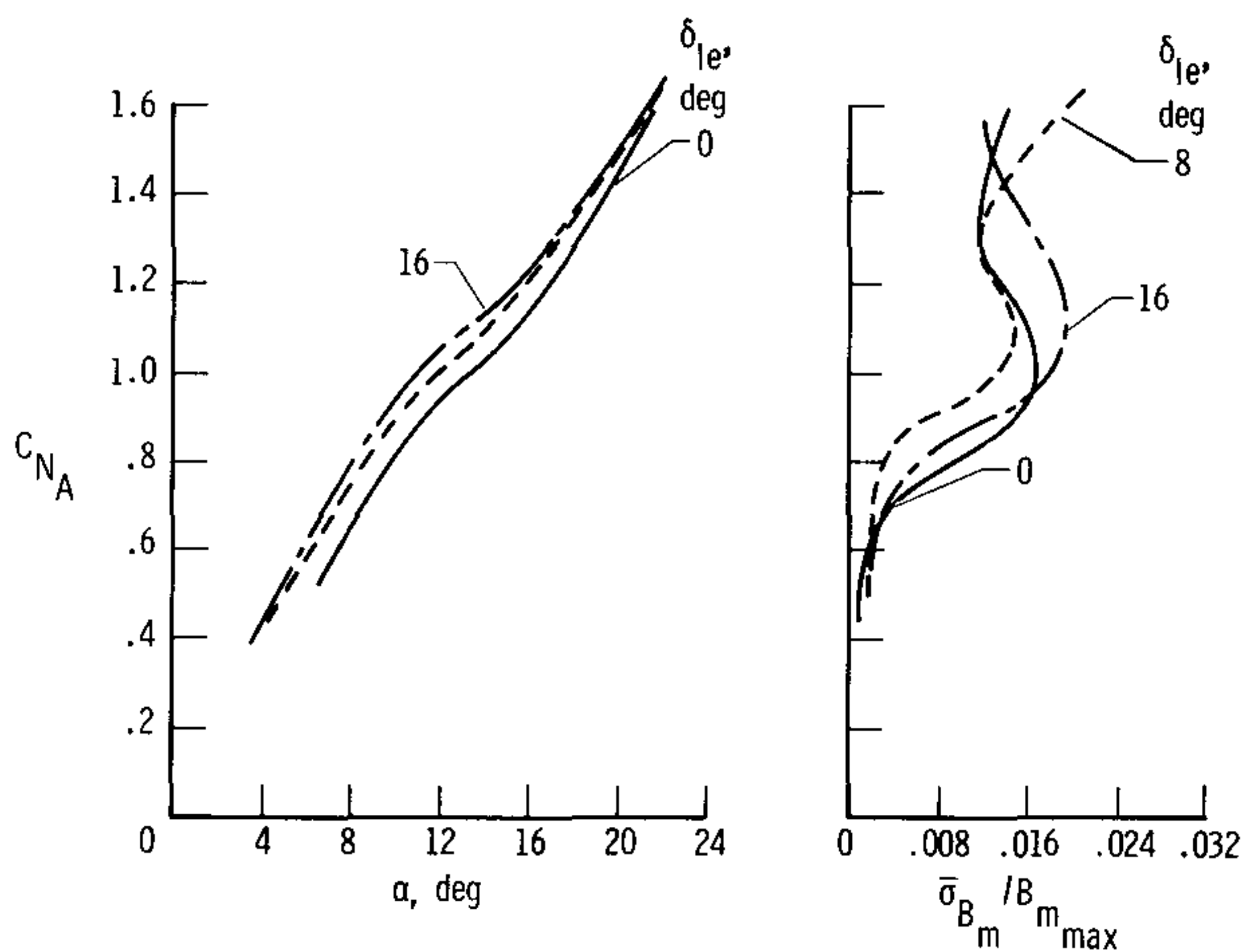
(d) Mach 0.85, scheduled leading-edge flaps, fixed trailing-edge flaps.

Figure 12. Concluded.
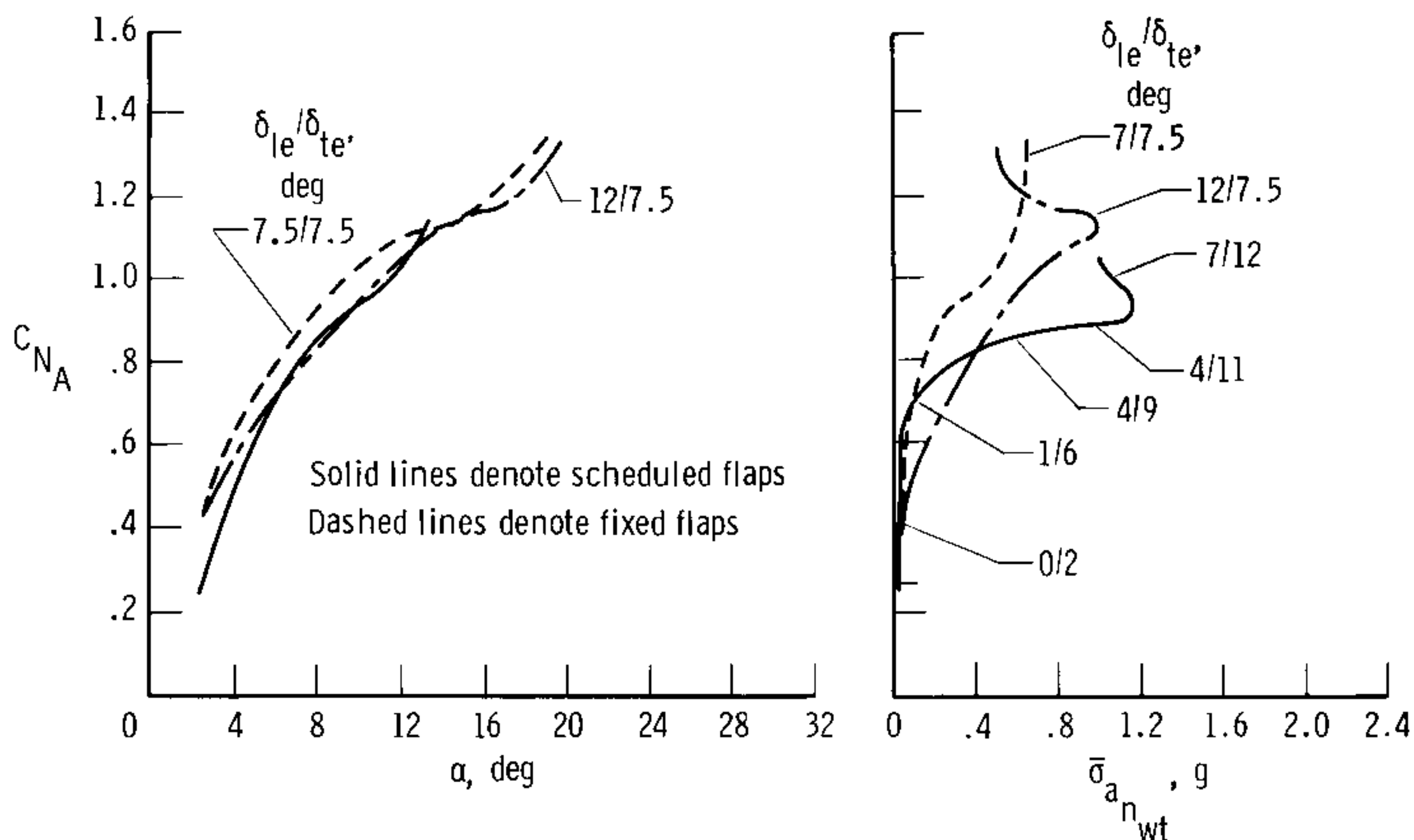
(a) Mach 0.80, δ_{te} = 7.5° except where scheduled.
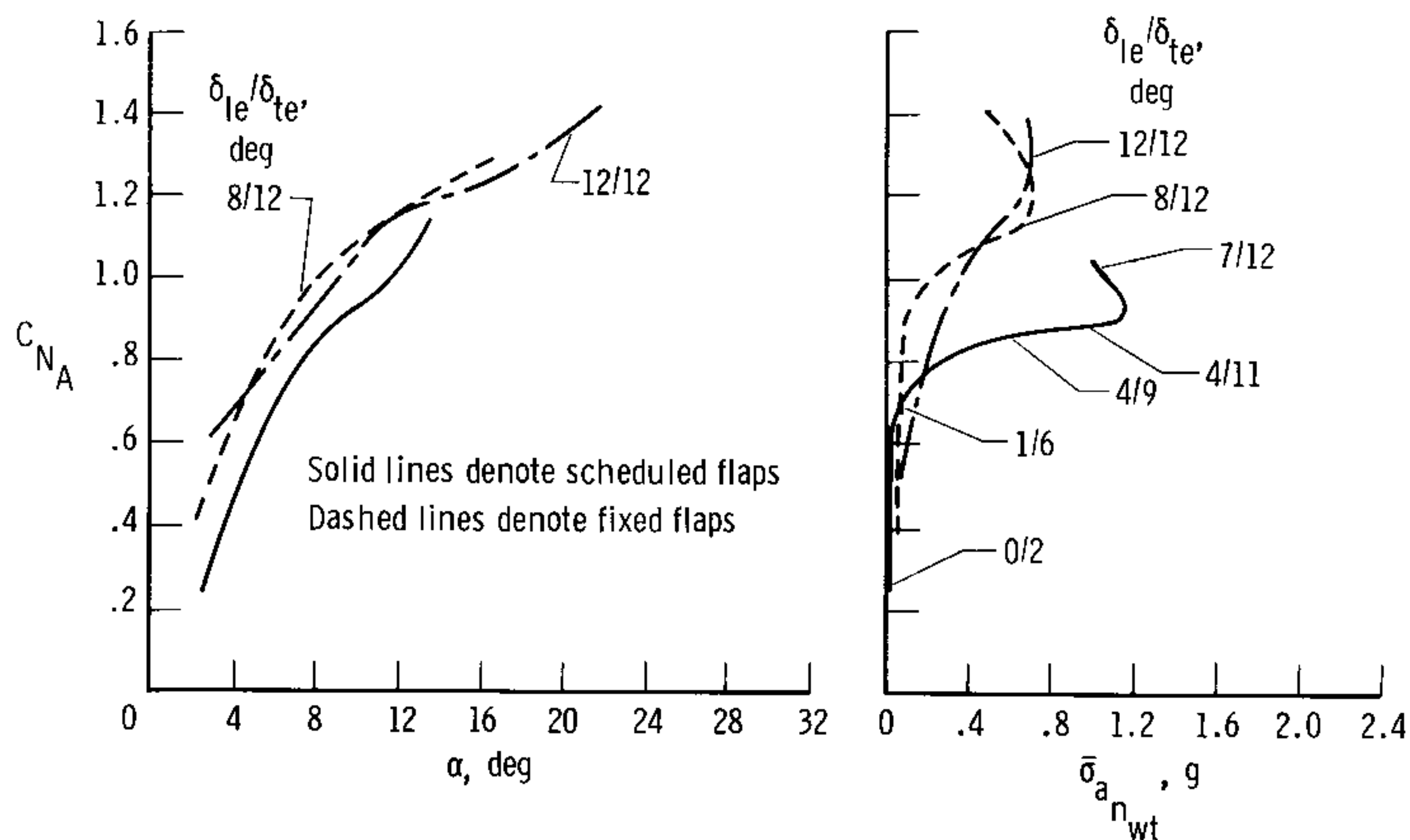
(b) Mach 0.80, δ_{te} = 12° except where scheduled otherwise.

Figure 13. Variation of YF-17 normal-force coefficients with angle of attack and buffet intensity for fixed and scheduled flaps.
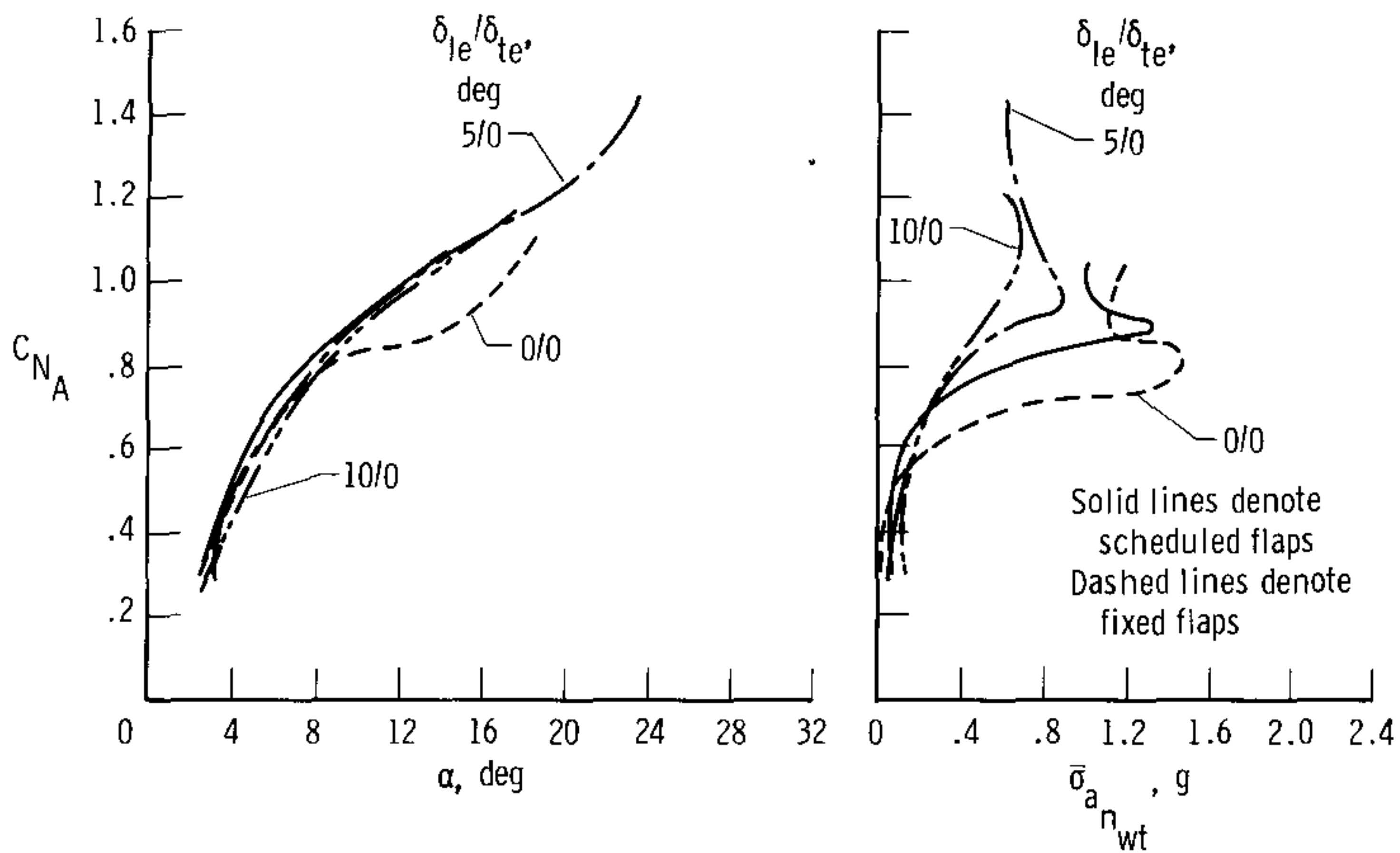
(c) Mach 0.90, $\delta_{te} = 0°$ except where scheduled.
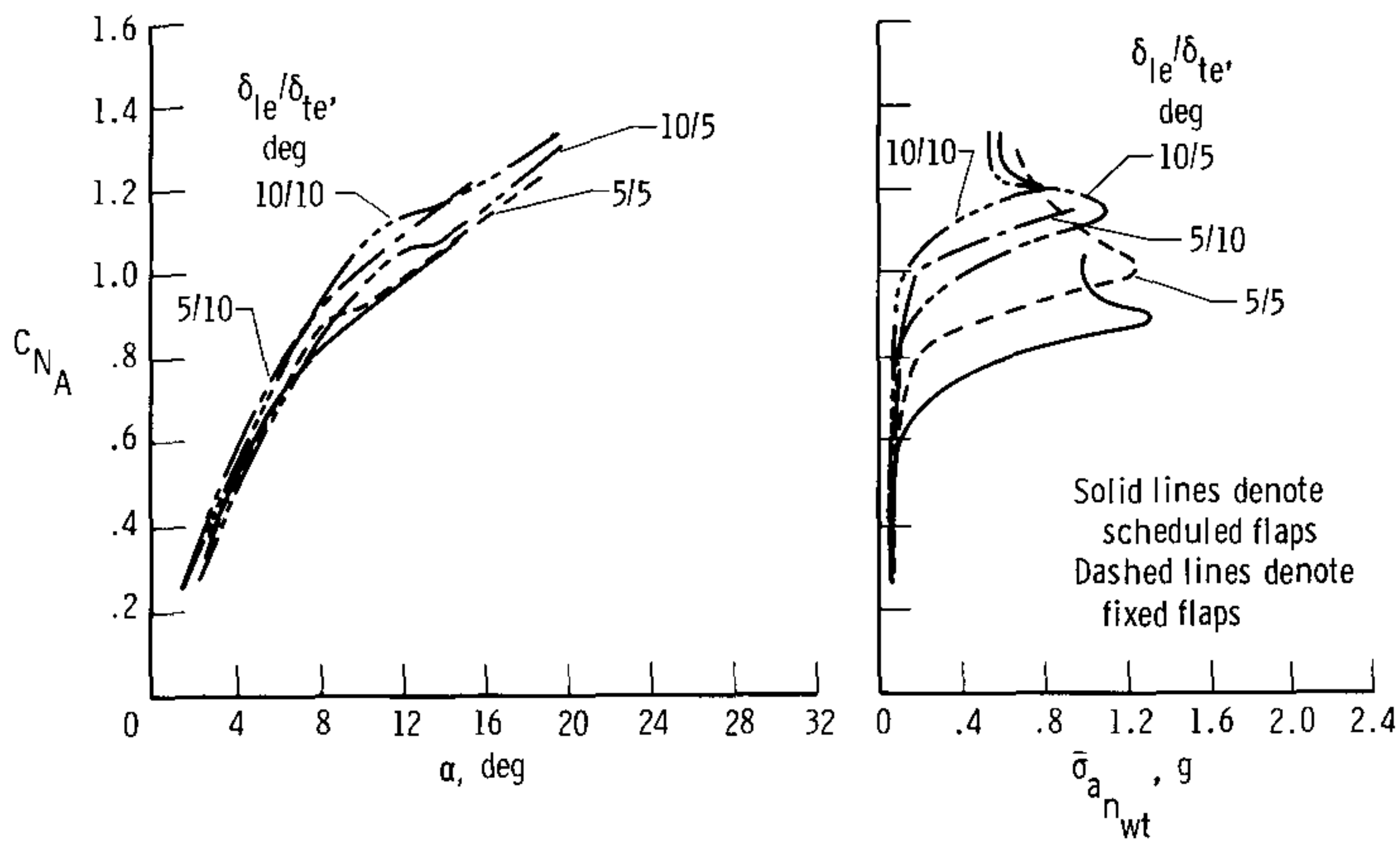
(d) Mach 0.90.

Figure 13. Concluded.
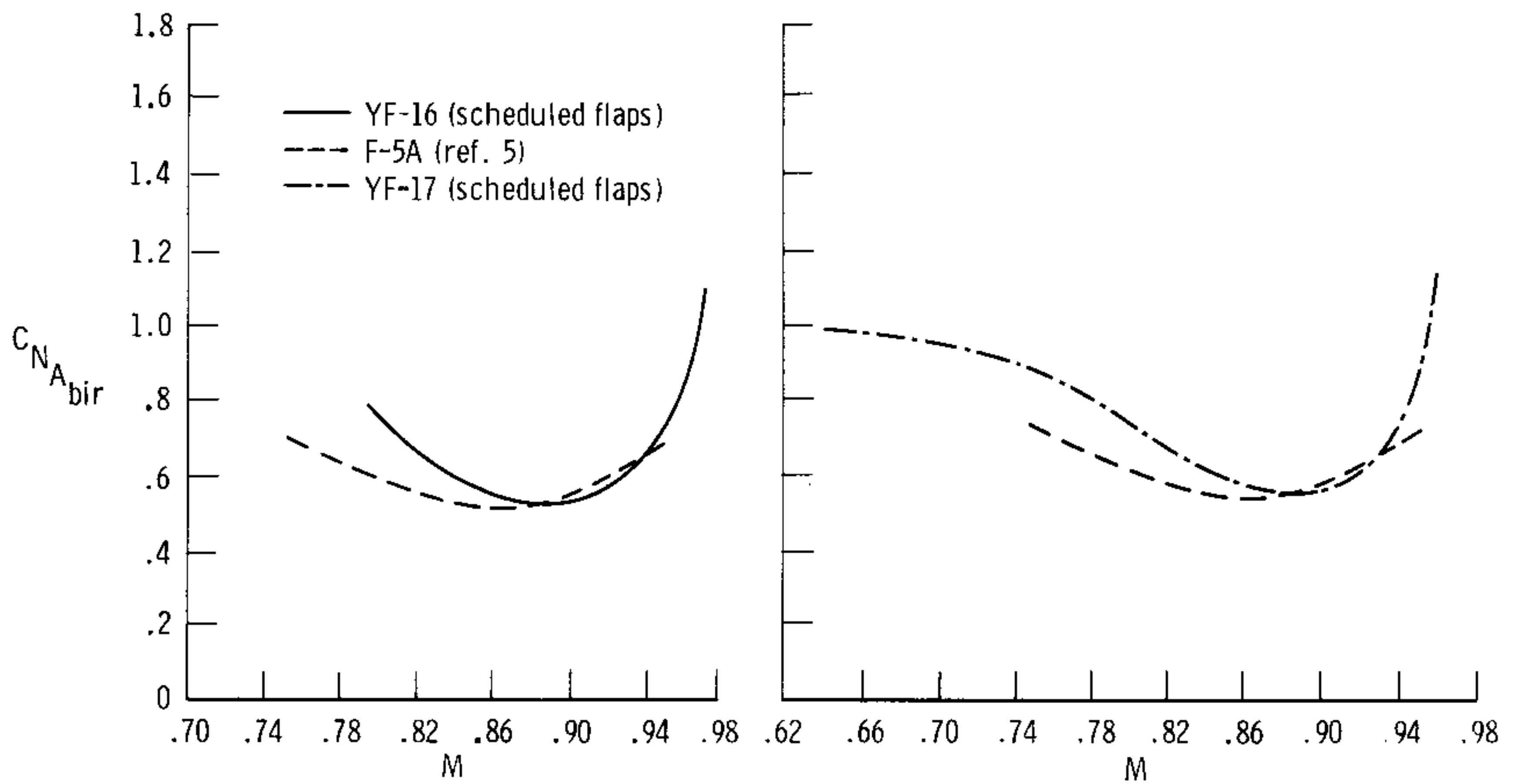
(a) Buffet intensity rise characteristics.

Figure 14. Comparison of lightweight fighter and F-5A aircraft buffet characteristics and normal-force curves.
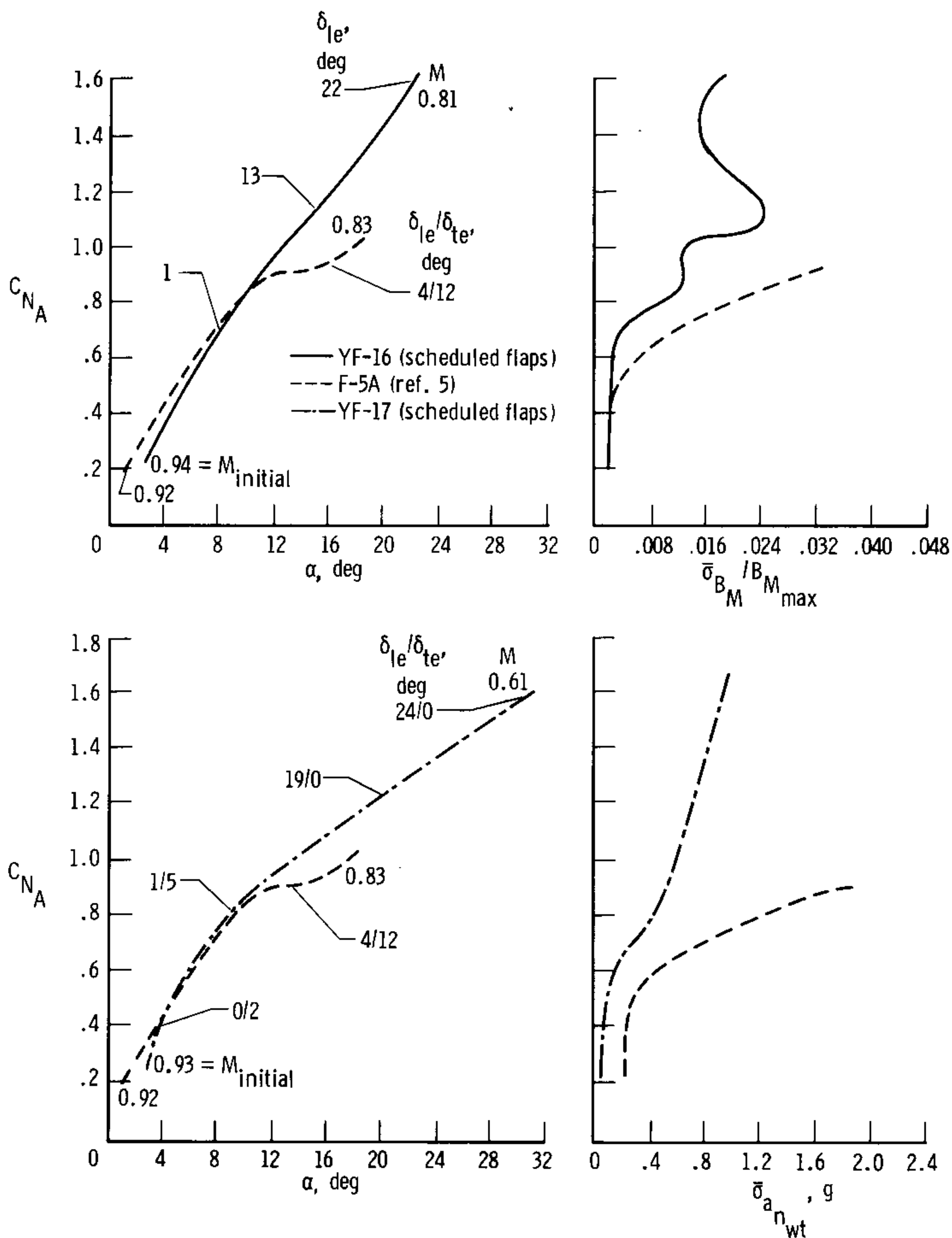
(b) *Normal-force curves and buffet intensity characteristics.*

Figure 14. Concluded.
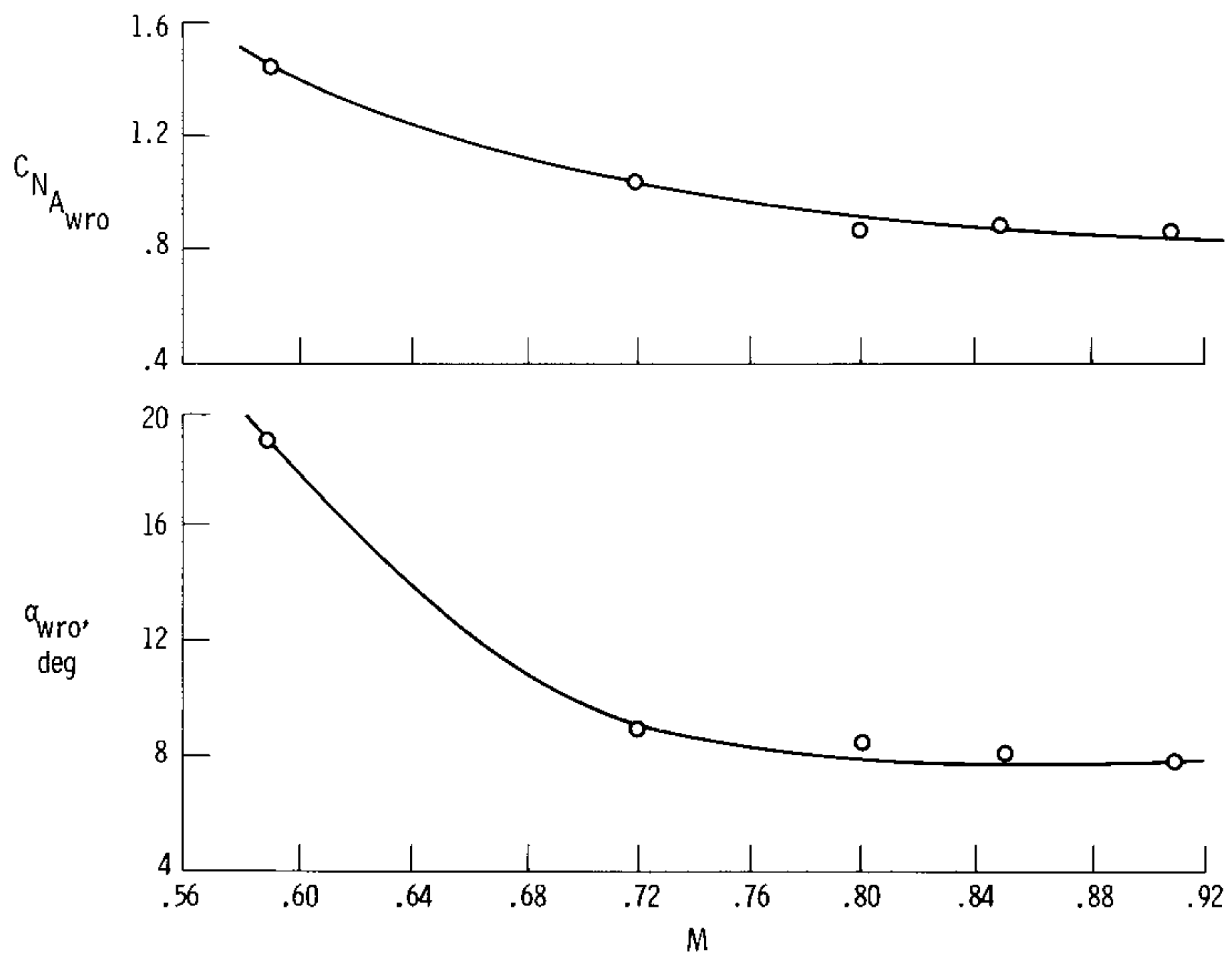
Figure 15. YF-17 wing rock onset boundaries with scheduled flaps.
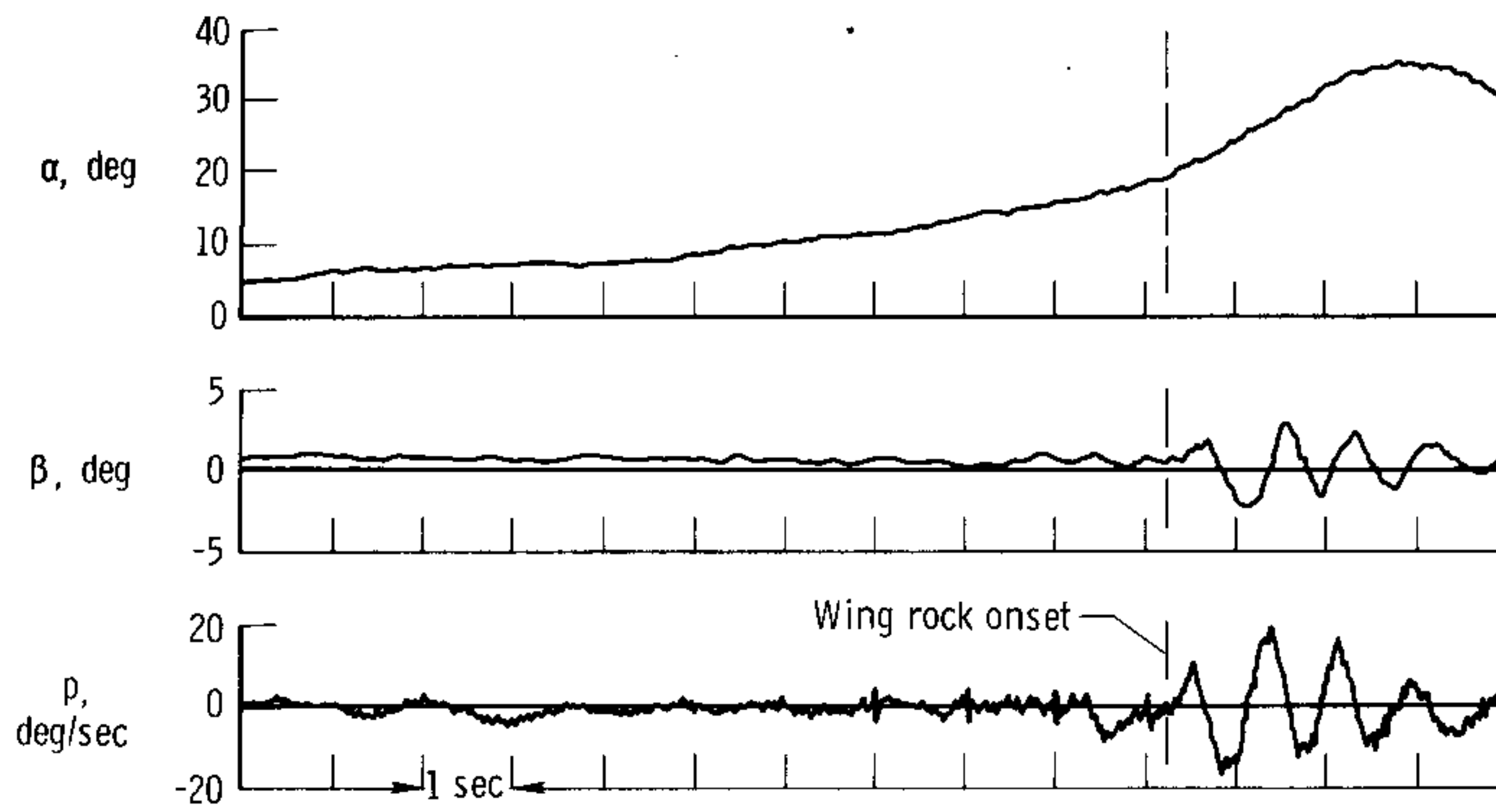
(a) Mach 0.60.
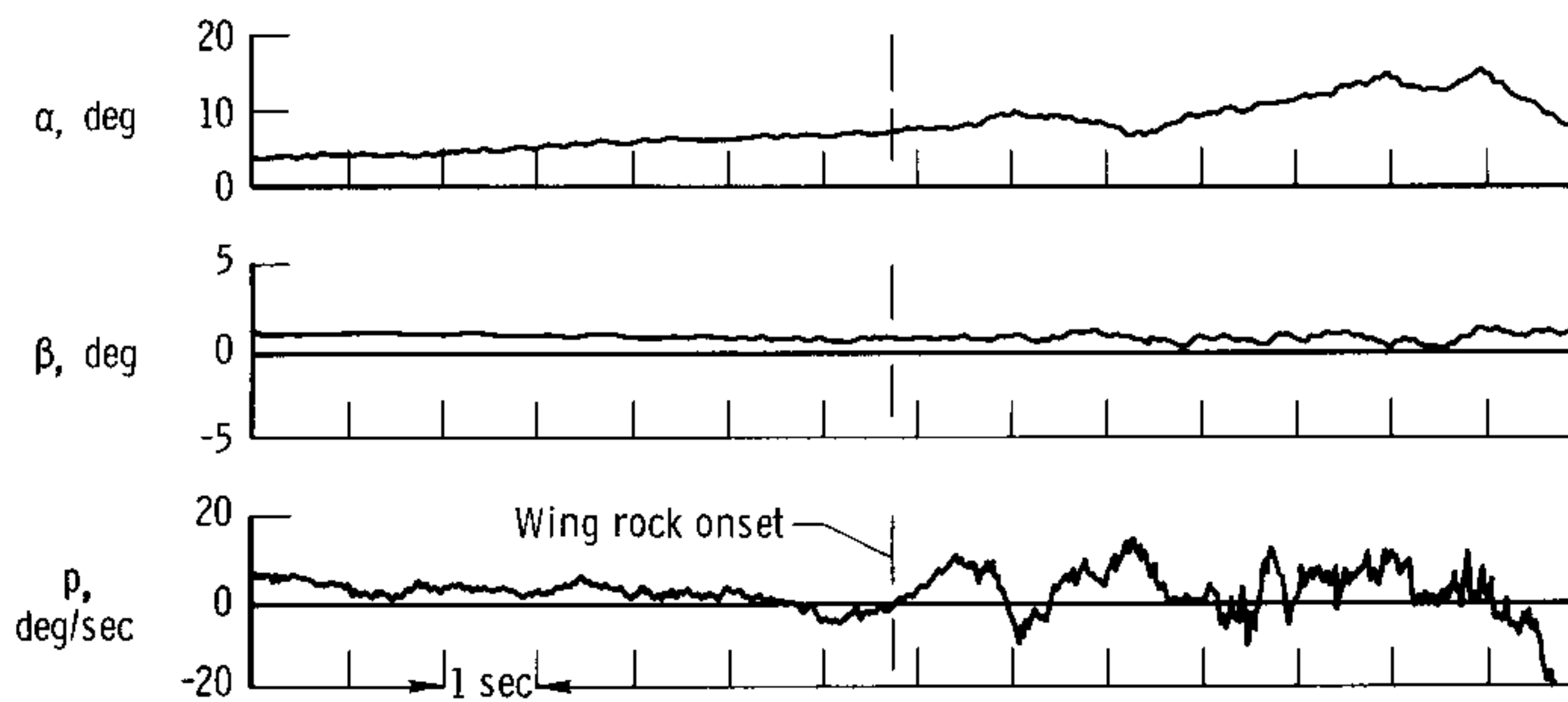
(b) Mach 0.85.

Figure 16. Typical YF-17 wing rock time histories.
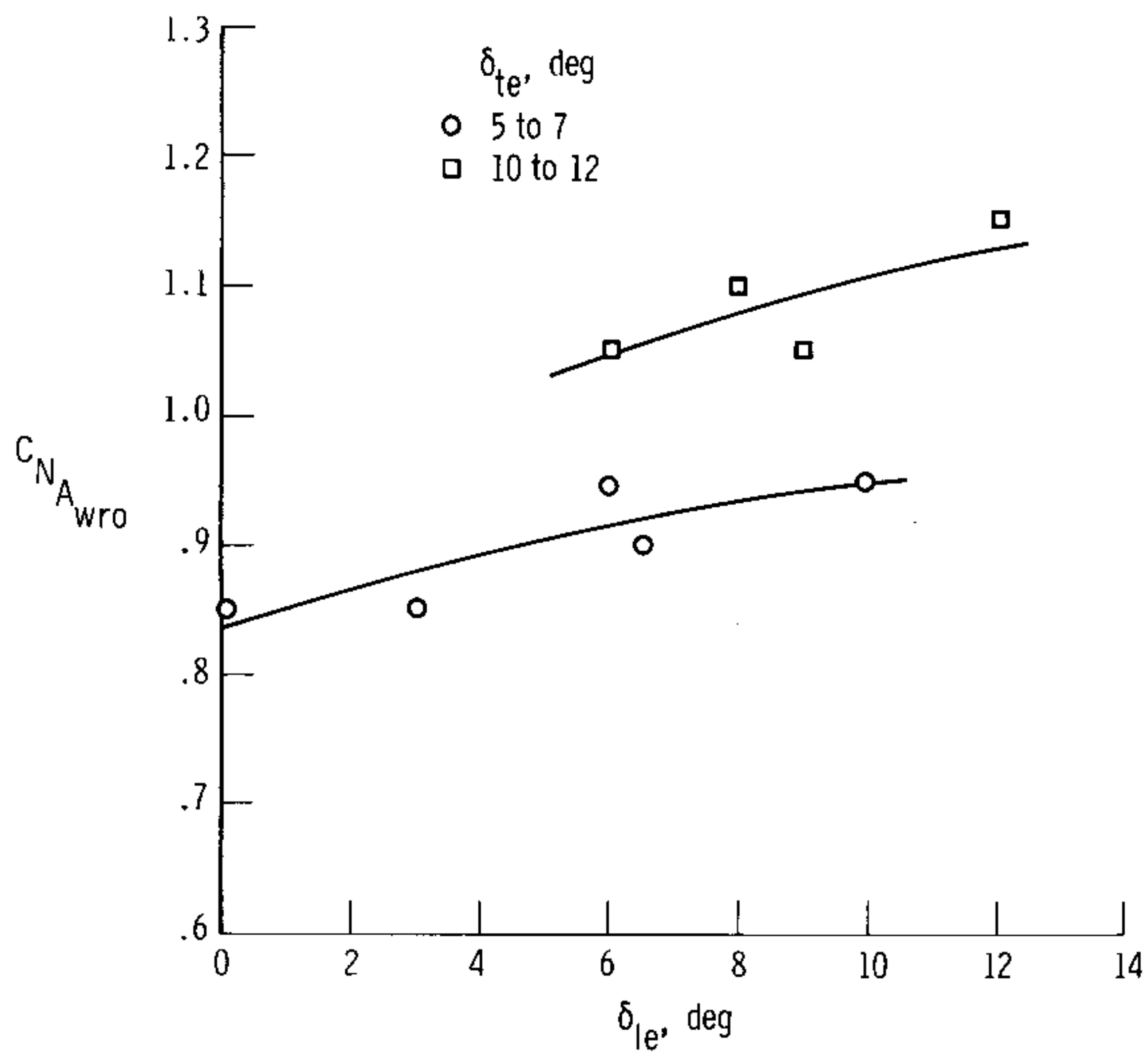
*Figure 17. YF-17 wing rock onset characteristics with fixed flaps.
Mach 0.80.*
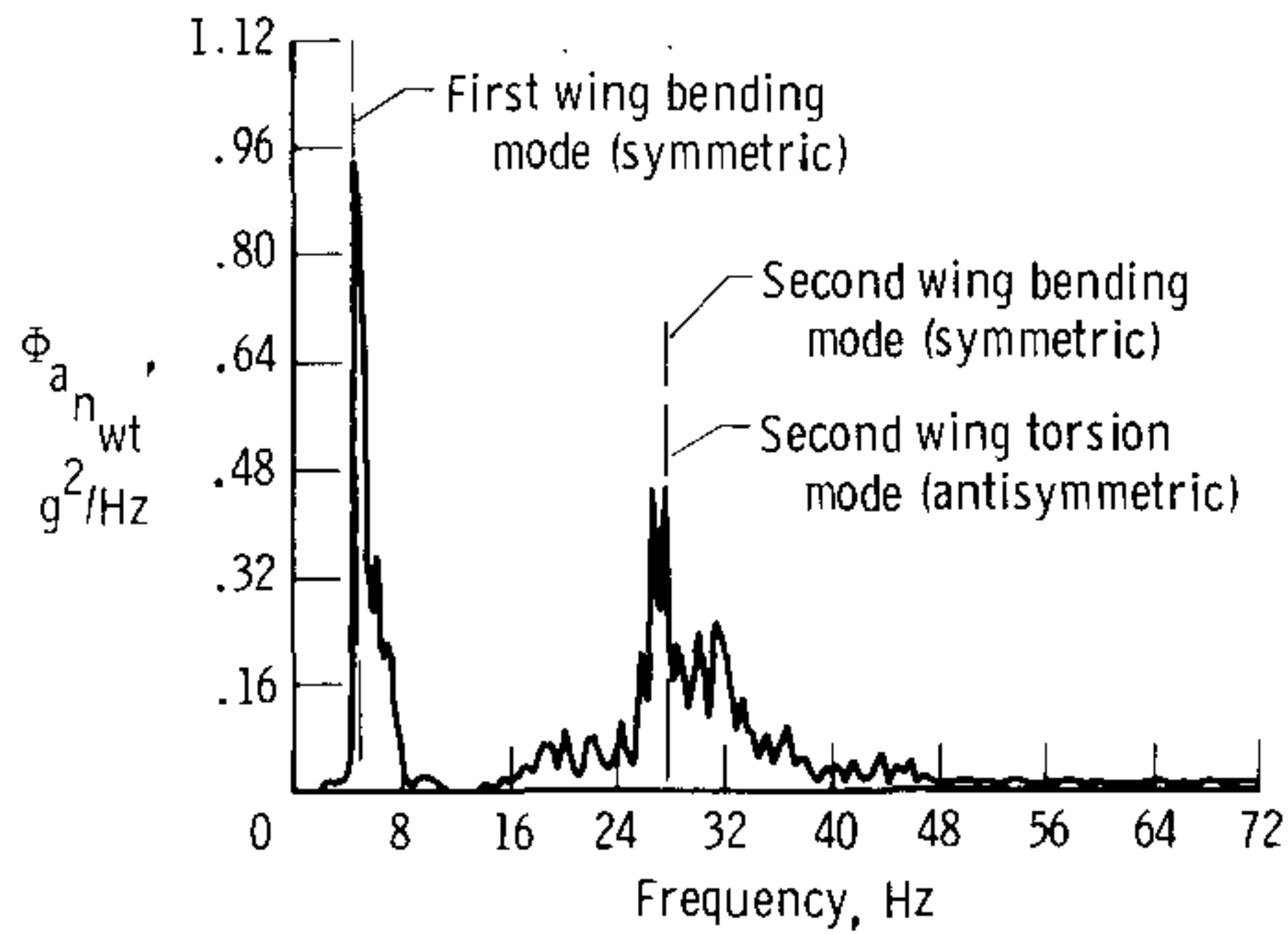
(a) YF-17 airplane, $M_{initial}$ = 0.85, $C_{N_{A_{initial}}}$ = 0.80,

scheduled flaps.
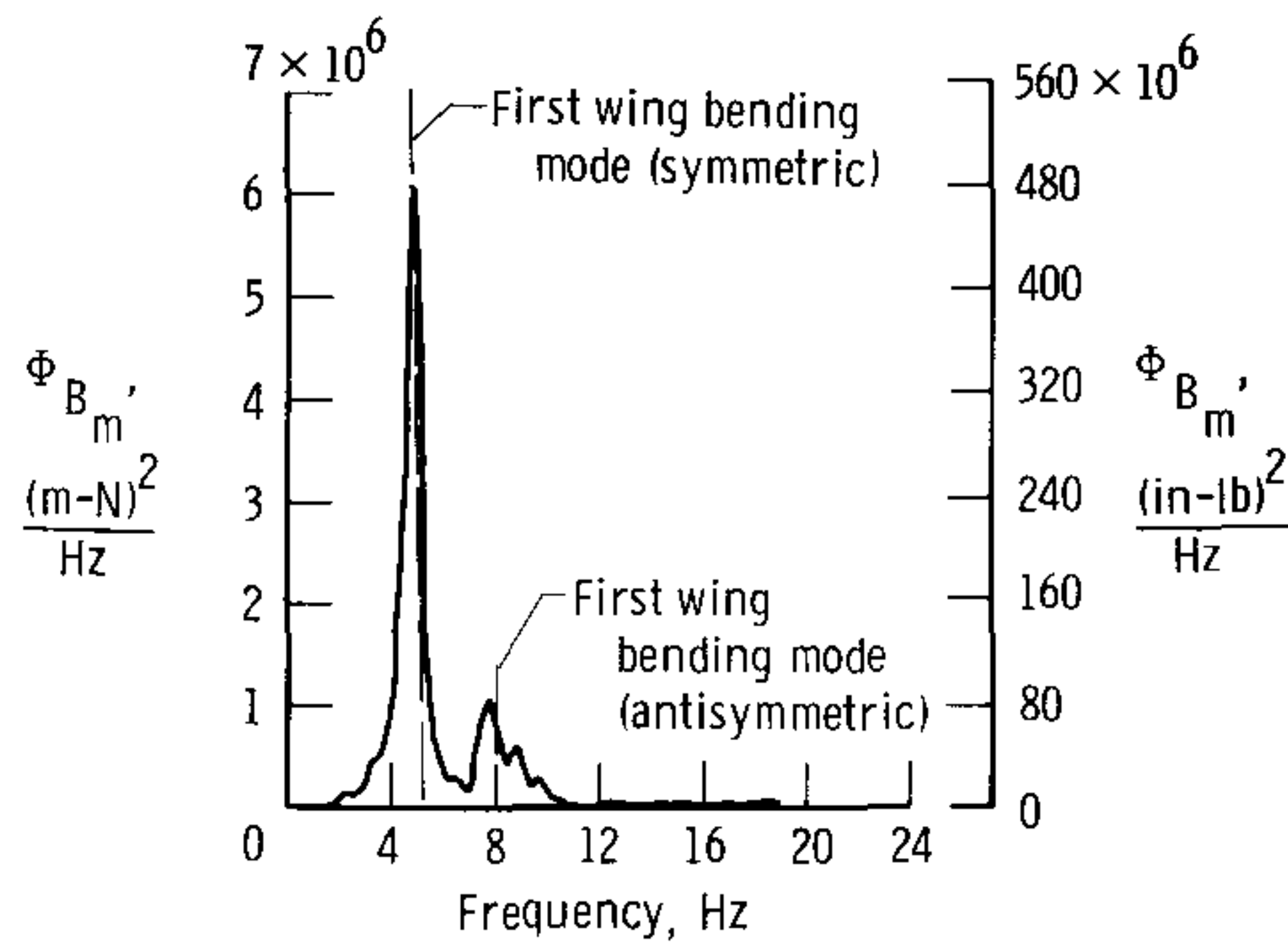
(b) YF-16 airplane, $M_{initial}$ = 0.87, $C_{N_{A_{initial}}}$ = 1.00,

scheduled leading-edge flaps.

Figure 18. Wing structural response characteristics.
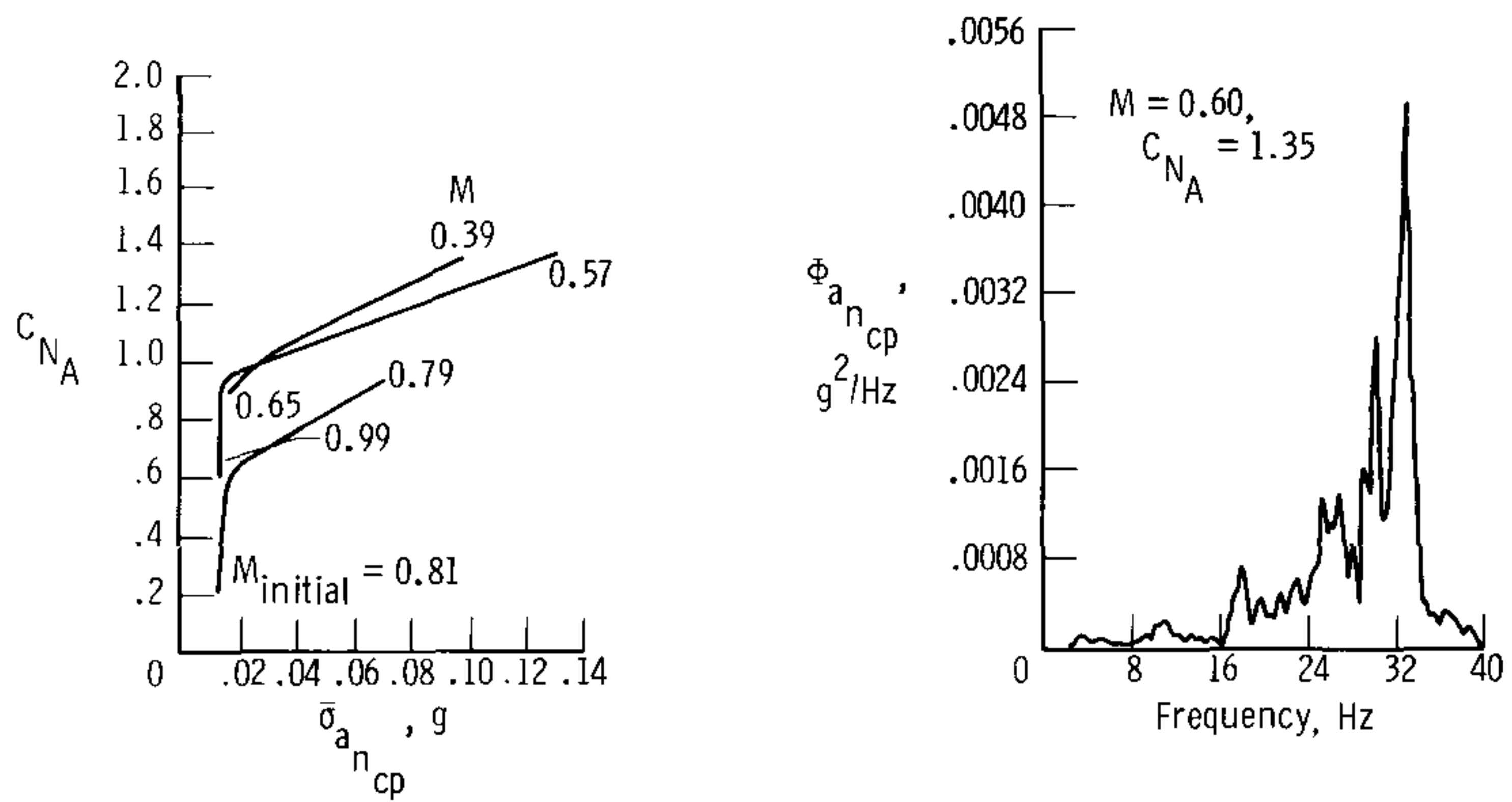
(a) YF-17 airplane.
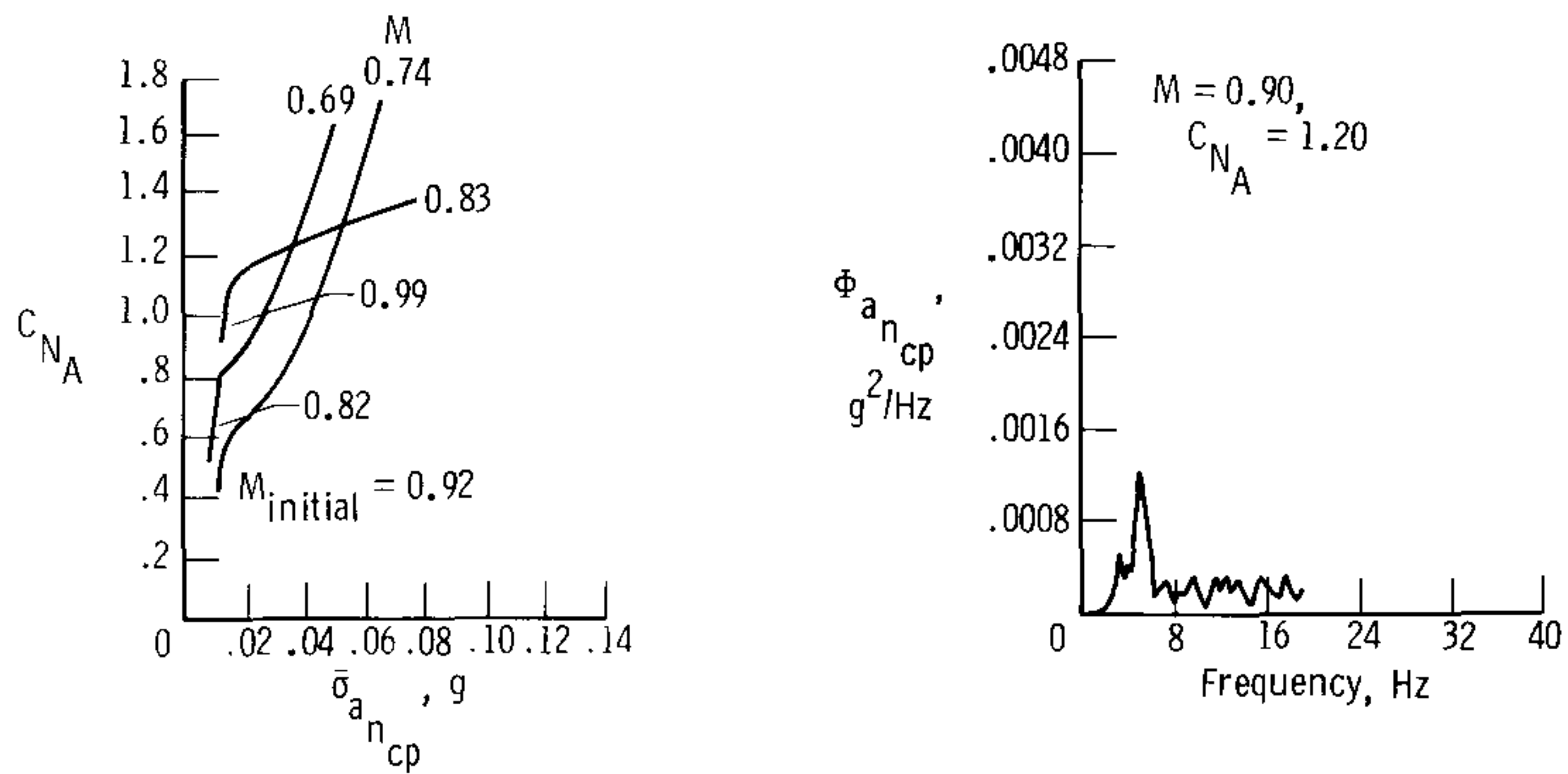
(b) YF-16 airplane.

Figure 19. Lightweight fighter cockpit buffet intensities and frequency distributions.
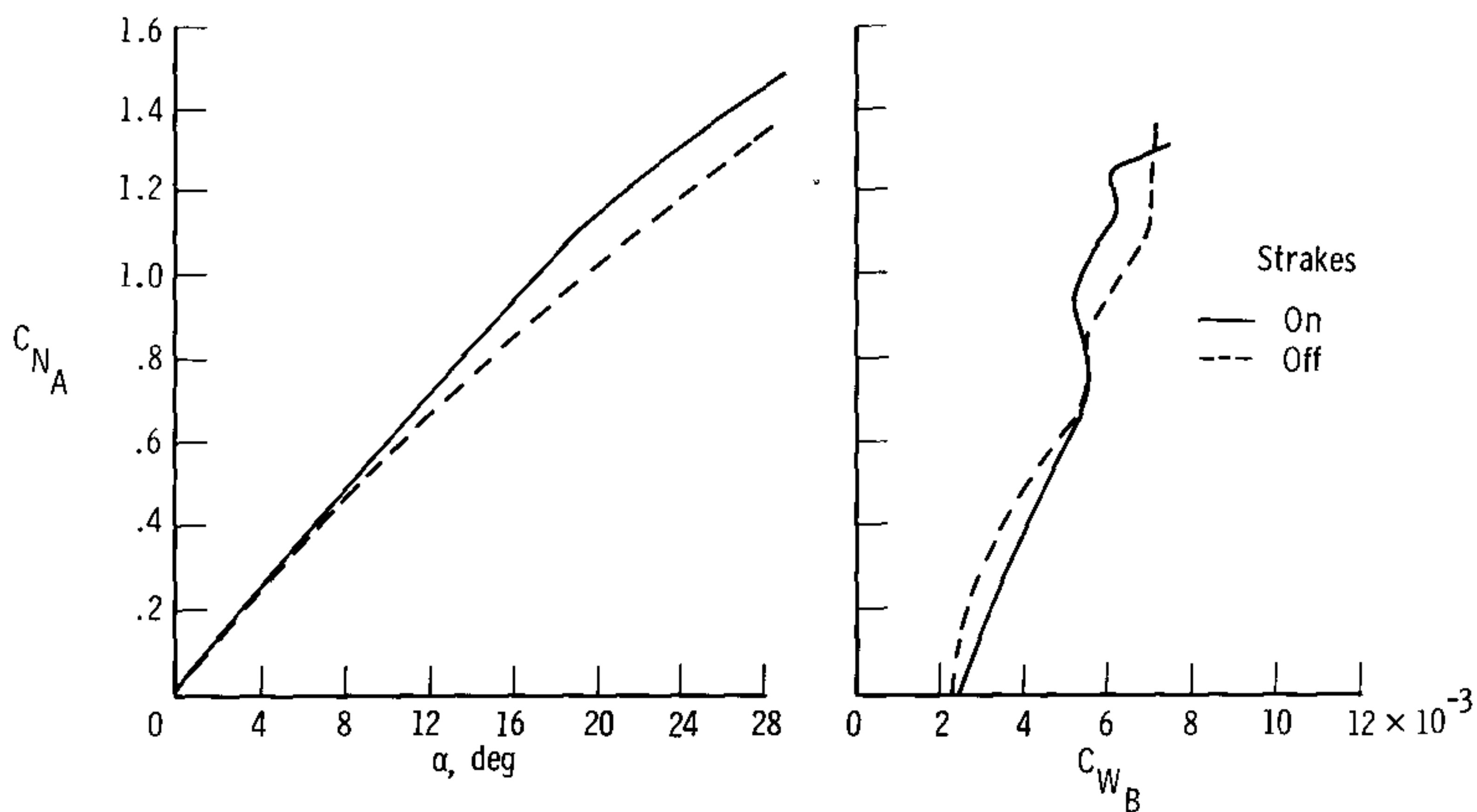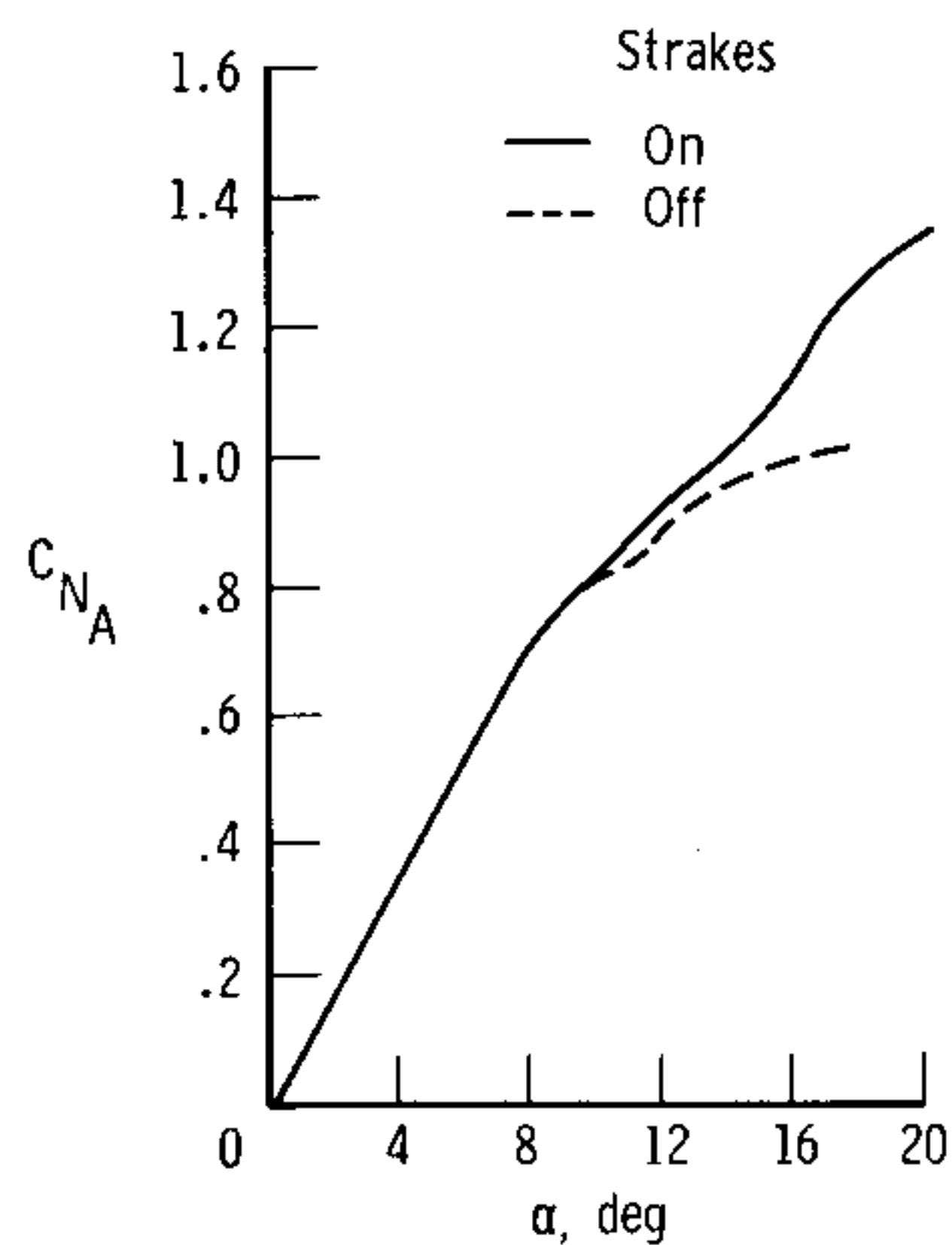
(a) Missiles and launchers off, clean wing.
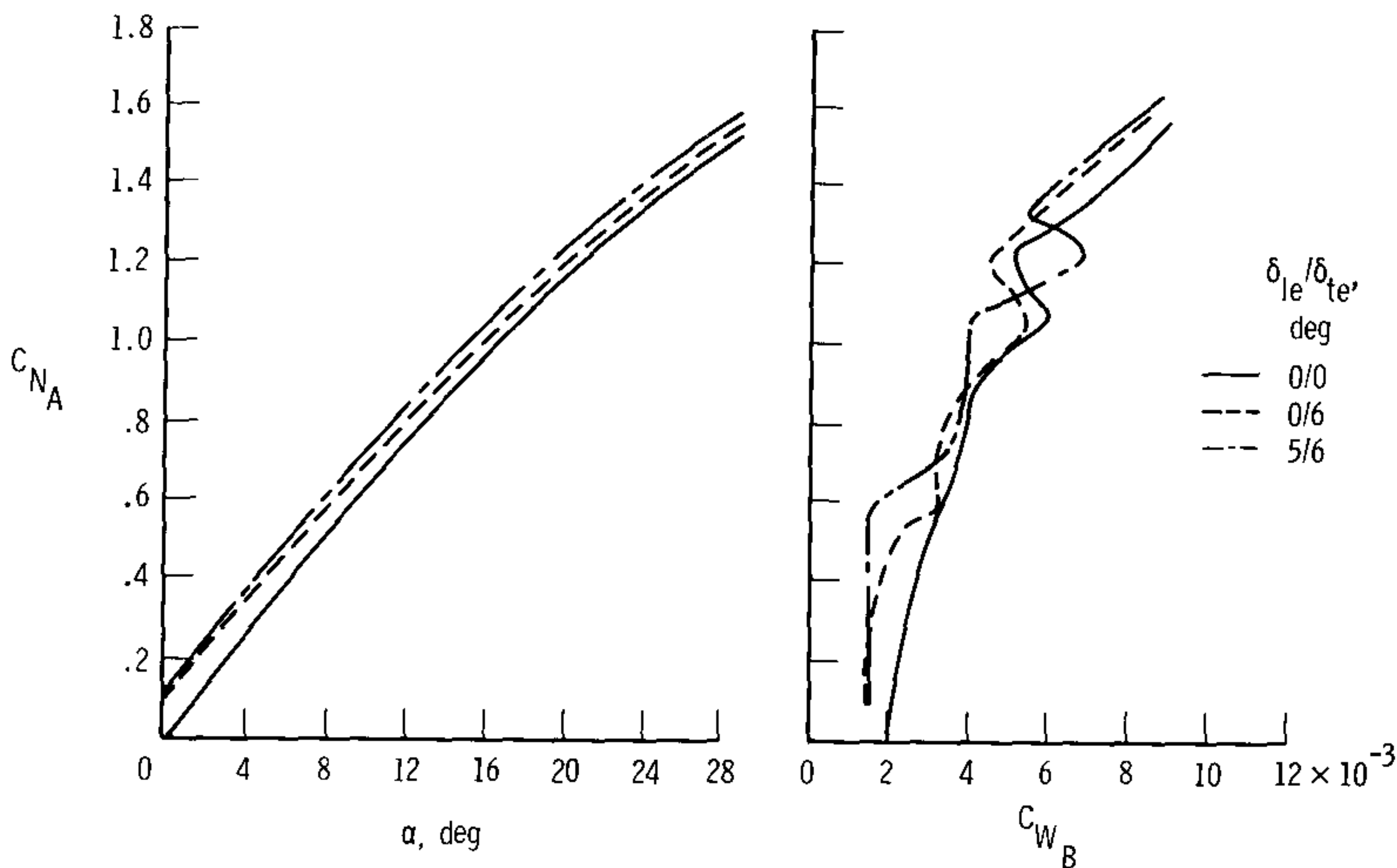
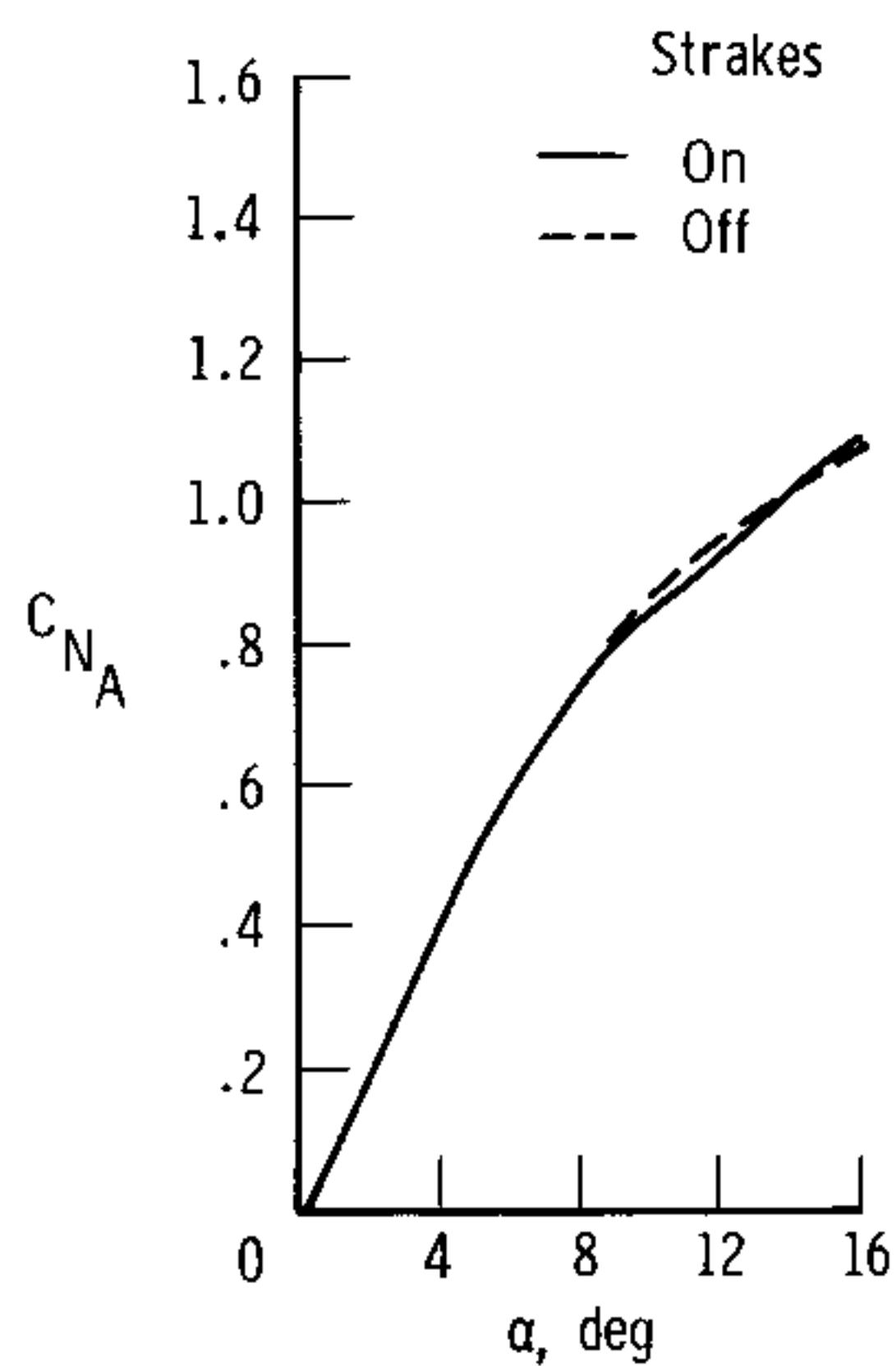(b) Strakes on, missiles and launchers on.

Figure 20. YF-16 wind tunnel model normal-force coefficients with and without forebody strakes and with fixed flaps. Mach 0.80.
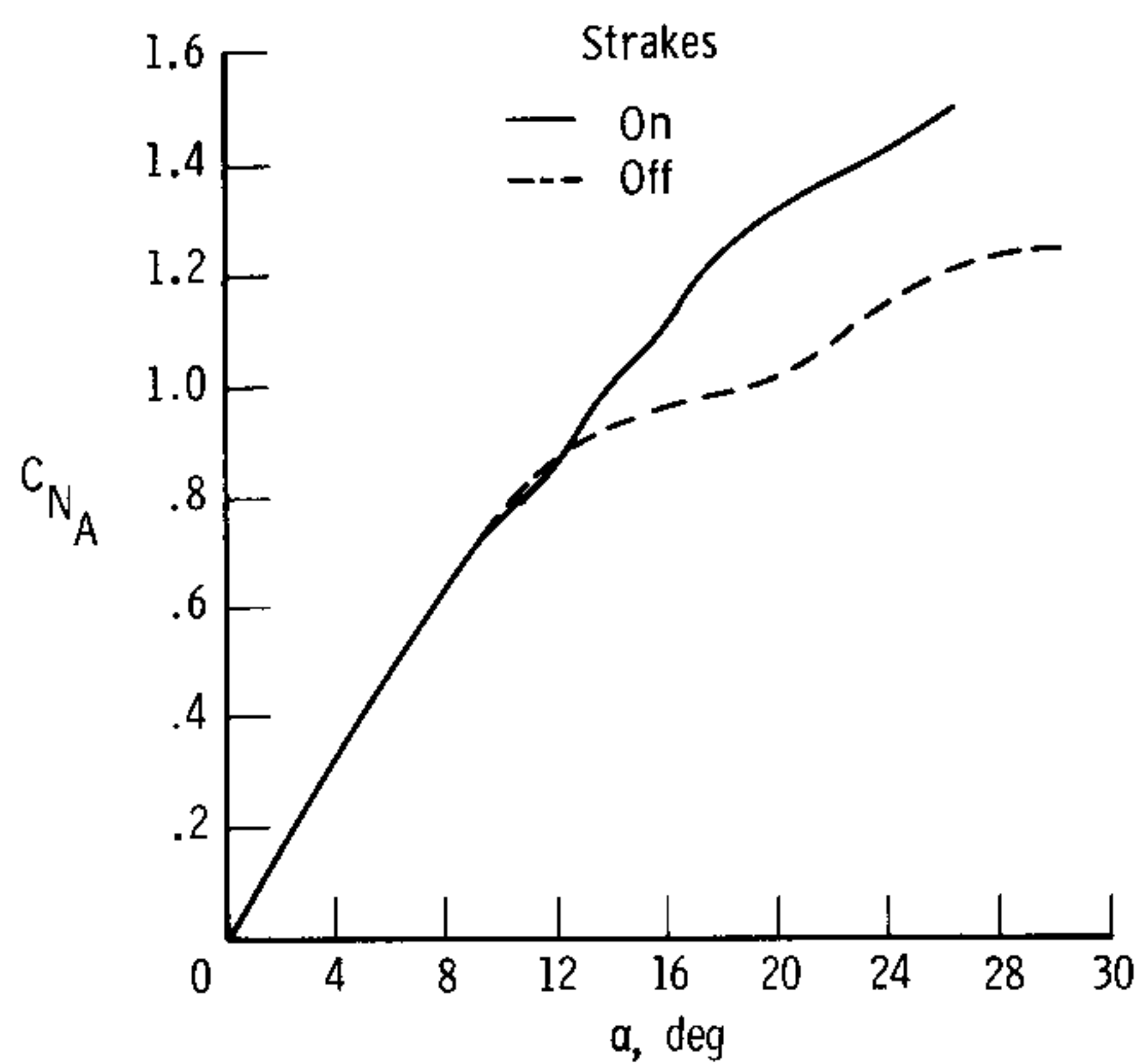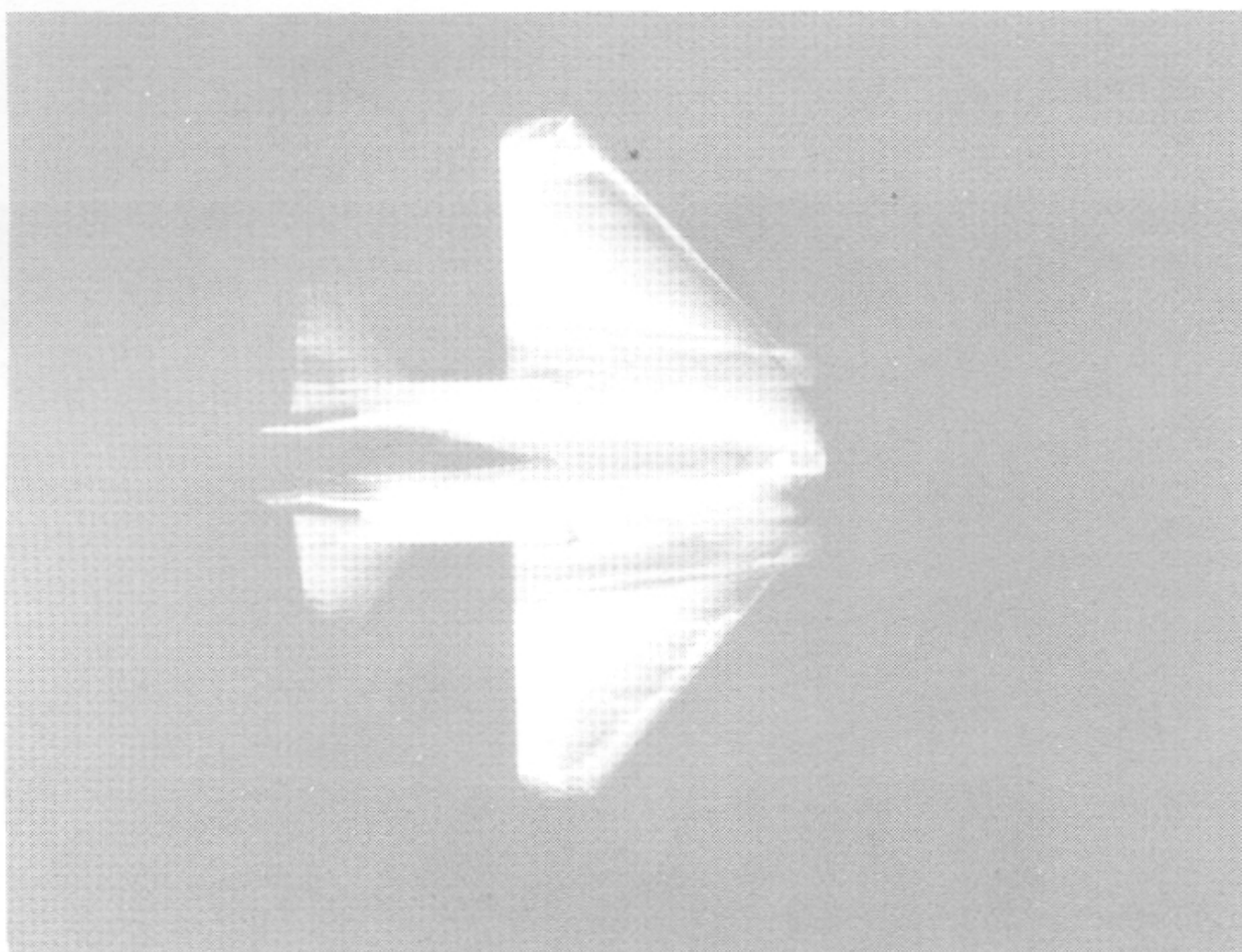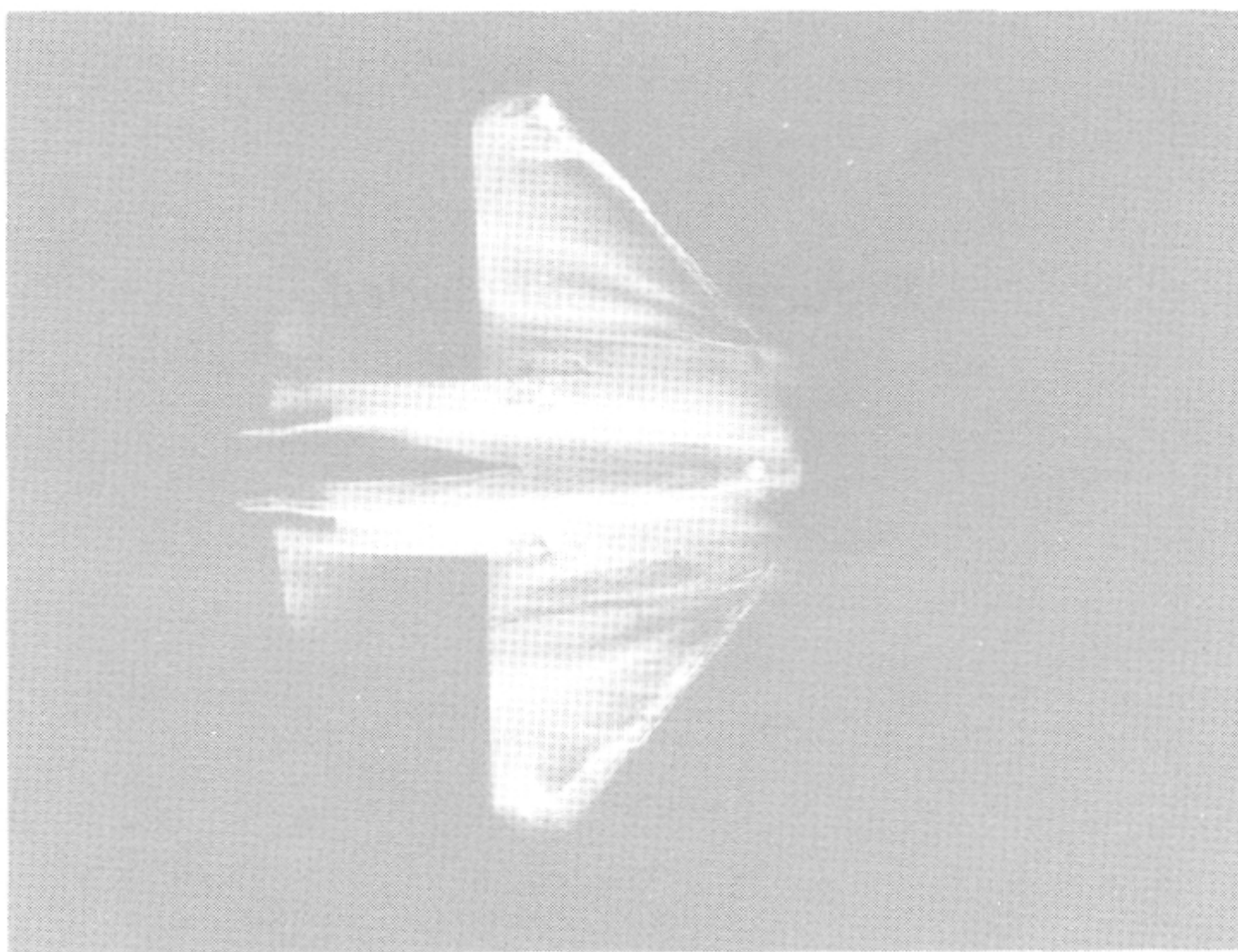
(a) Mach 0.60.

(b) Mach 0.80.

(c) Mach 0.90.

Figure 21. YF-17 wind tunnel model normal-force coefficients with and without forebody strakes for clean wing.

(a) C_{N_A} = 0.44, α = 4.7°.

(b) C_{N_A} = 0.87, α = 10.8°.

Figure 22. Oil flow photographs of a 1/15-scale YF-16 model illustrating vortex flow due to strakes and regions of separated flow. Upper wing surface; Mach 0.90.

(c) C_{N_A} = 1.27, α = 16.7°.

Figure 22. Concluded.

"The aeronautical and space activities of the United States shall be conducted so as to contribute . . . to the expansion of human knowledge of phenomena in the atmosphere and space. The Administration shall provide for the widest practicable and appropriate dissemination of information concerning its activities and the results thereof."

—NATIONAL AERONAUTICS AND SPACE ACT OF 1958

NASA SCIENTIFIC AND TECHNICAL PUBLICATIONS

TECHNICAL REPORTS: Scientific and technical information considered important, complete, and a lasting contribution to existing knowledge.

TECHNICAL NOTES: Information less broad in scope but nevertheless of importance as a contribution to existing knowledge.

TECHNICAL MEMORANDUMS: Information receiving limited distribution because of preliminary data, security classification, or other reasons.

CONTRACTOR REPORTS: Scientific and technical information generated under a NASA contract or grant and considered an important contribution to existing knowledge.

TECHNICAL TRANSLATIONS: Information published in a foreign language considered to merit NASA distribution in English.

SPECIAL PUBLICATIONS: Information derived from or of value to NASA activities. Publications include conference proceedings, monographs, data compilations, handbooks, sourcebooks, and special bibliographies.

TECHNOLOGY UTILIZATION PUBLICATIONS: Information on technology used by NASA that may be of particular interest in commercial and other non-aerospace applications. Publications include Tech Briefs, Technology Utilization Reports and Notes, and Technology Surveys.

Details on the availability of these publications may be obtained from:

SCIENTIFIC AND TECHNICAL INFORMATION OFFICE

NATIONAL AERONAUTICS AND SPACE ADMINISTRATION
Washington, D.C. 20546